

# A retake on the analysis of scores truncated by terminal events

Klaus Kähler Holst<sup>1</sup>, Andreas Nordland<sup>1</sup>, Julie Furberg<sup>1</sup>,  
Lars Holm Damgaard<sup>1</sup>, Christian Bressen Pipper<sup>1,2</sup>

<sup>1</sup>Novo Nordisk, Søborg, Denmark

<sup>2</sup>Department of Public Health, Epidemiology, Biostatistics and Biodemography,  
University of Southern Denmark, Odense, Denmark

February 11, 2025

## Abstract

Analysis of data from randomized controlled trials in vulnerable populations requires special attention when assessing treatment effect by a score measuring, e.g., disease stage or activity together with onset of prevalent terminal events. In reality, it is impossible to disentangle a disease score from the terminal event, since the score is not clinically meaningful after this event. In this work, we propose to assess treatment interventions simultaneously on disease score and the terminal event. Our proposal is based on a natural data-generating mechanism respecting that a disease score does not exist beyond the terminal event. We use modern semi-parametric statistical methods to provide robust and efficient estimation of the risk of terminal event and expected disease score conditional on no terminal event at a pre-specified landmark time. We also use the simultaneous asymptotic behavior of our estimators to develop a powerful closed testing procedure for confirmatory assessment of treatment effect on both onset of terminal event and level of disease score. A simulation study mimicking a large-scale outcome trial in chronic kidney patients as well as an analysis of that trial is provided to assess performance.

**Key Words:** randomized trial, causal inference, terminal event, truncation

## 1 Introduction

Clinical scores of organ conditions or physical ability are not meaningful beyond events such as organ replacement therapy or death. Consequently, in trials where such terminal events are prevalent, this should be reflected by statistical methods that target the impact of the treatment intervention on disease scores.

A number of established strategies have been developed to address truncation of measurements due to death or another terminal event. These fall into three broad categories:

- 1: Evaluate treatment effect in a scenario where you imagine you can intervene to prevent any terminal events prior to time of evaluation.
- 2: Evaluate treatment effect assigning a worst possible value to initially planned measurements beyond the terminal event.
- 3: Evaluate treatment effect conditional on no terminal event.

The first strategy employs assumptions to predict how measurements post terminal events would behave had the terminal events not occurred. That is, it treats measurements truncated by

terminal events as ordinary missing data that can be handled using specific missing at random or missing not at random assumptions (Diggle et al., 2002). The resulting estimated treatment effect reflects treatment intervention in a scenario where the terminal event can be prevented in the whole target population. If, in reality, this is not feasible another strategy needs to be considered (Kahan et al., 2020).

The second strategy incorporates risk of terminal event in the assessment through an utility framework where scores are assigned an unfavorable value after the terminal event to enforce a penalty due to event in the assessment of treatment interventions. Effectively what is done here is to translate the cost of a terminal event to an unfavorable number on the measurement scale. The choice of an unfavorable value is clearly a discussion point as it may ultimately govern conclusions about treatment effect (Kurland and Heagerty, 2005).

The third strategy can be pursued in a number of distinct ways. Approaches include the pattern mixture approach (Fitzmaurice and Laird, 2000), principal stratification (Frangakis et al., 2007), while without terminal event approaches (Lin, 2003), terminal decline approaches (Chan and Wang, 2010), and finally the partially conditional approach (Kurland and Heagerty, 2005). For an in depth discussion of these approaches and their relative merits we refer the reader to Kurland et al. (2009).

We provide an extension of the partially conditional approach advocated in Kurland and Heagerty (2005) to enable a natural, efficient, and assumption lean assessment of the effect of treatment interventions simultaneously on both the disease score and the onset of a terminal event. Importantly, this is accomplished without making assumptions about the behavior of disease score after terminal event had the event not occurred nor is it required to equate such measurements to an unfavorable number on the disease score scale.

Our proposal is focused around large scale randomized controlled trials in vulnerable populations where a surrogate marker along with a prevalent terminal event forms the basis of evaluating treatment effect. In particular we are motivated by the recently conducted FLOW trial (Perkovic et al., 2024). FLOW was a double-blind randomized controlled trial. The trial objective was to investigate the ability of semaglutide - a once weekly glucagon like peptide-1 receptor agonist - to delay progression of kidney disease in a population with type 2 diabetes and chronic kidney disease at high risk of kidney disease progression.

A major challenge in this study was a substantial number of terminal events at any relevant landmark time after randomization (Perkovic et al., 2024). We will assess performance of our proposal in a simulation study mimicking the FLOW trial as well as analyse the actual trial data according to our proposal.

The paper is structured as follows. we introduce the formal set up and define the mathematical notation and the target parameters In Section 2. Section 3 is dedicated to deriving the efficient influence function for these target parameters together with efficient estimators based on working prediction models for the nuisance components. A closed testing procedure for simultaneous assessment of effect on both the disease score scale and the risk of terminal event is outlined in Section 4. We present a Monte Carlo simulation study cast over the FLOW trial in Section 5 and proceed with an analysis of the FLOW data in Section 6. Finally, a discussion and directions for future research is outlined in Section 7.

## 2 Setup and notation

We consider a setup where the occurrence events in scope and the value of the measurement of interest are evaluated at some landmark time  $\tau$  after randomization to treatment  $A$ . In this context, we denote the first occurrence of an event that invalidates the measurement of interest by  $T^*$ . Several distinct types of events may occur at this time and we denote the specific types by  $\epsilon^*$ . We assume that among these types of events, the event of interest for the evaluation of the treatment effect at  $\tau$  is encoded as  $\epsilon^* = 1$ . The subjects in the trial may also drop-out at some time-point after randomization either due to trial closeout or for other reasons. We denote this censoring time by  $C$  and let  $T = T^* \wedge C$  denote the first time either censoring or an event

occurs, where  $\wedge$  denotes the minimum operator. We also let  $\Delta = I(T^* \leq C)$  denote the indicator of whether censoring or an event is observed, and let  $\epsilon = \epsilon^* \Delta$  be the observed cause of failure subject to right-censoring.

Furthermore, in the scenario  $T^* \geq \tau$  where a meaningful clinical measurement of interest exists, we denote this measurement by  $Y$ . We note that in this scenario  $Y$  may not be observed either due to censoring before  $\tau$ , ( $C < \tau$ ), or if measurement is not obtained for other reasons. We let  $R$  be the indicator of whether  $Y$  is observed ( $R = 1$ ) or not ( $R = 0$ ). We note that with this notation  $R = 1$  entails  $T > \tau$ .

In this setup, we envisage a treatment intervention  $A = a$  where we observe the counterfactuals  $T^{*(a)}$  and  $\epsilon^{*(a)}$  as well as the counterfactual  $Y^{(a)}$  when  $T^{*(a)} \geq \tau$ . Our assessment of treatment effects will then naturally evolve around contrasting the following two quantities across treatment interventions:

$$\theta_{T^*}^{(a)} = \mathbb{P} \left( T^{*(a)} \leq \tau, \epsilon^{*(a)} = 1 \right), \quad (1)$$

$$\theta_{Y|T^*}^{(a)} = \mathbb{E} \left[ Y^{(a)} \mid T^{*(a)} > \tau \right]. \quad (2)$$

The contrasts we consider in this context are given by:

$$\begin{aligned} \psi_{T^*} &= \theta_{T^*}^{(0)} - \theta_{T^*}^{(1)}, \\ \psi_{Y|T^*} &= \theta_{Y|T^*}^{(1)} - \theta_{Y|T^*}^{(0)}. \end{aligned}$$

Note that a positive value of  $\psi_{T^*}$  entails a reduction in the risk of event of interest at time  $\tau$  due to treatment. In addition, a positive value of  $\psi_{Y|T^*}$  entails a treatment-induced increase in the expected value of the clinical measurement at time  $\tau$  among the subset of patients where this measurement is meaningful.

Given this interpretation, the benefits of a treatment intervention are naturally assessed by means of  $\psi_{T^*}$  and  $\psi_{Y|T^*}$ . This interpretation clearly comes with the cautionary note that due to competing risks, a reduction in risk of event of interest could potentially be caused by an increase in risk of competing events Putter et al. (2007).

Considering for instance chronic kidney disease, a drug is deemed beneficial if we can claim no clinically relevant elevated risk of kidney failure due to treatment (under the implicit assumption that treatment does increase the risk of death from other causes) and in addition a treatment-induced improvement in kidney function among those that are still alive and have not had kidney failure at time  $\tau$ . If we formalize this statement it exactly corresponds to simultaneously testing the two null-hypotheses

$$H_{Y|T^*} : \psi_{Y|T^*} \leq \delta_{Y|T^*} \text{ and } H_{T^*} : \psi_{T^*} \leq -\delta_{T^*}$$

For some superiority margin  $\delta_{Y|T^*} \geq 0$  and some non-inferiority margin  $\delta_{T^*} \geq 0$ . Note that for  $\delta_{Y|T^*} = \delta_{T^*} = 0$  this corresponds to classical testing for superiority of treatment.

We revisit the testing procedures for this testing problem in Section 4.

## 2.1 Assumptions and Identification

In order to enable the assessment above we need to be able to identify and estimate the targeted treatment contrasts from the observed data. For this purpose, we further introduce a set of baseline covariates denoted by  $X$ .

The baseline covariates are utilized to formulate a set of missing data assumptions that will enable identification in combination with standard exchangeability and consistency assumptions. In addition, to allow for reliable estimation, we are going to make a number of positivity assumptions and assume that the randomized treatment is independent of the baseline covariates. Below, we list the assumptions.

(A1) Treatment randomization

$$A \perp\!\!\!\perp X$$

(A2) Exchangeability

$$Y^{(a)}, T^{*(a)}, \epsilon^{*(a)} \perp\!\!\!\perp A$$

(A3) Consistency

$$T^{*(a)} = T^*, \epsilon^{*(a)} = \epsilon^*, Y^{(a)} = Y \text{ when } A = a$$

(A4) Missing at random (outcome)

$$Y \perp\!\!\!\perp R \mid T^* > \tau, A$$

(A5) Random censoring (time to event)

$$T^*, \epsilon^* \perp\!\!\!\perp C \mid A$$

(A6) Positivity

$$\mathbb{P}(R = 1 \mid A = a, X = x) > 0 \forall a, x$$

(A7) Positivity (censoring)

$$\mathbb{P}(C > \tau \mid A = a) > 0 \forall a$$

Based on the above assumptions we are able to identify  $\theta_{Y|T^*}^{(a)}$  from the observed data through the expectation  $\mathbb{E}\{I(A = a) \cdot R \cdot Y\}$  and  $P(R = 1, A = a)$  as follows:

$$\begin{aligned} \theta_{Y|T^*}^{(a)} &= \mathbb{E}\left[Y^{(a)} \mid T^{*(a)} > \tau\right] \\ &\stackrel{(A2)}{=} \mathbb{E}\left[Y^{(a)} \mid T^*(a) > \tau, A = a\right] \\ &\stackrel{(A3)}{=} \mathbb{E}\left[Y \mid T^* > \tau, A = a\right] \\ &\stackrel{(A4)}{=} \frac{\mathbb{E}\left[R \cdot Y \mid T^* > \tau, A = a\right]}{\mathbb{P}\left(R = 1 \mid T^* > \tau, A = a\right)} \\ &\stackrel{R=1 \Rightarrow T^* > \tau}{=} \frac{\mathbb{E}\left[I(A = a) \cdot R \cdot Y\right]}{\mathbb{P}\left(R = 1, A = a\right)} \end{aligned}$$

Similarly, we are able to identify  $\theta_{T^*}^{(a)}$  from the observed data through the cause-specific hazard  $\mathbb{P}(T = t, \epsilon = 1, \Delta = 1 \mid T \geq t, A = a)$ , the all-cause (including censoring) survival  $\mathbb{P}(T \geq t \mid A = a)$ , and the censoring distribution  $\mathbb{P}(C \geq t \mid A = a)$ . The actual identification steps are given below:

$$\begin{aligned}
\theta_{T^*}^{(a)} &= \mathbb{P}\left(T^{*(a)} \leq \tau, \epsilon^{*(a)} = 1\right) \\
&= \int_0^\tau \mathbb{P}\left(T^{*(a)} = t, \epsilon^{*(a)} = 1\right) dt \\
&\stackrel{(A2)}{=} \int_0^\tau \mathbb{P}\left(T^{*(a)} = t, \epsilon^{*(a)} = 1 \mid A = a\right) dt \\
&\stackrel{(A3)}{=} \int_0^\tau \mathbb{P}\left(T^* = t, \epsilon^* = 1 \mid A = a\right) dt \\
&\stackrel{(A5)}{=} \int_0^\tau \mathbb{P}\left(T^* = t, \epsilon^* = 1 \mid C \geq t, A = a\right) dt \\
&= \int_0^\tau \mathbb{P}\left(T^* = t, \epsilon^* = 1 \mid T^* \geq t, C \geq t, A = a\right) \mathbb{P}\left(T^* \geq t \mid C \geq t, A = a\right) dt \\
&= \int_0^\tau \mathbb{P}\left(T = t, \epsilon = 1, \Delta = 1 \mid T \geq t, A = a\right) \frac{\mathbb{P}\left(T \geq t \mid A = a\right)}{\mathbb{P}\left(C \geq t \mid A = a\right)} dt
\end{aligned}$$

As for the treatment randomization assumption and the positivity assumptions, these are utilized in the next section, where we develop estimation procedures.

### 3 Estimation

#### 3.1 Deriving the Efficient Influence Function for $\theta_{Y|T^*}^{(a)}$

We first note, that due to the treatment randomization assumption (A1), the log-likelihood for the observed data,  $Z = (Y, R, A, X)$ , has the following decomposition

$$\log\{f(Y \mid R, A, X)\} + \log\{f(R \mid A, X)\} + \log\{f(A)\} + \log\{f(X)\}.$$

It follows that the tangent space as a subspace of the Hilbert space of  $L_{P_0}^2$  zero mean functions endowed with covariance inner product is given by

$$\mathcal{T} = \mathcal{T}_1 \oplus \mathcal{T}_2 \oplus \mathcal{T}_3 \oplus \mathcal{T}_4,$$

where

$$\begin{aligned}
\mathcal{T}_1 &= \{h(Y, R, A, X) \in \mathcal{H} \mid \mathbb{E}[h(Y, R, A, X) \mid R, A, X] = 0\}, \\
\mathcal{T}_2 &= \{h(R, A, X) \in \mathcal{H} \mid \mathbb{E}[h(R, A, X) \mid A, X] = 0\}, \\
\mathcal{T}_3 &= \{h(A) \in \mathcal{H} \mid \mathbb{E}[h(A)] = 0\}, \\
\mathcal{T}_4 &= \{h(X) \in \mathcal{H} \mid \mathbb{E}[h(X)] = 0\},
\end{aligned}$$

and all sets are considered subsets of square-integrable functions with zero mean. First note that

$$\mathcal{T}_1^\perp \cap \mathcal{T}_2^\perp = \{h(A, X) \in \mathcal{H} \mid \mathbb{E}[h(A, X)] = 0\}.$$

Along the lines of Zhang et al. (2008), the orthogonal complement to the full tangent space is therefore determined as

$$\mathcal{T}^\perp = (\mathcal{T}_1^\perp \cap \mathcal{T}_2^\perp) \cap (\mathcal{T}_3^\perp \cap \mathcal{T}_4^\perp) = \{h(A, X) \in \mathcal{H} \mid \mathbb{E}[h(A, X) \mid X] = 0\}.$$

As  $A$  is binary with  $\pi_a(P_0) = \mathbb{P}(A = a)$ , we see that

$$\mathcal{T}^\perp = \{(A - \pi_1)h(X) \mid \mathbb{E}[h(X)^2] < \infty\}. \quad (3)$$

We note that under the missing at random assumption ( $A_4$ ) the target parameter is identified from the observed data as

$$\theta_{Y|T^*}^{(a)}(P) = \mathbb{E}_P \left[ \frac{I(A=a)R}{\mathbb{P}_P(A=a, R=1)} Y \right],$$

the strategy for finding an efficient estimator for  $\theta_{Y|T^*}^{(a)}(P_0)$  is first to find a consistent estimator (but not necessarily efficient one) and then project the corresponding influence function onto the tangent space. The resulting influence function is the efficient influence function, from which a locally efficient estimator can be obtained, which we describe in more detail in Section 3.3. For the first step, a consistent estimator for  $\theta_{Y|T^*}^{(a)}(P_0)$  is immediately obtained from the plugin (inverse probability weighting) estimator

$$\tilde{\theta}_{Y|T^*}^{(a)} = \mathbb{P}_n \frac{I(A=a, R=1)}{\mathbb{P}_n I(R=1, A=a)} Y, \quad (4)$$

which has influence function

$$\tilde{\phi}_{Y|T^*}^{(a)}(Z; P) = \frac{I(A=a)R}{\mathbb{P}_P(A=a)\mathbb{P}_P(R=1|A=a)} \{Y - \theta_{Y|T^*}^{(a)}(P)\}.$$

The EIF is now derived as

$$\phi_{Y|T^*}^{(a)}(Z; P) = \tilde{\phi}_{Y|T^*}^{(a)}(Z; P) - \Pi \left( \tilde{\phi}_{Y|T^*}^{(a)}(Z; P) \mid \mathcal{T}^\perp \right)$$

Let  $\rho_a(P) = \mathbb{P}_P(R=1|A=a)$ . The projection term is calculated as follows. An element in  $\mathcal{T}^\perp$  has the form  $(A - \pi_1)h(X)$  for an arbitrary element  $h$ . We need to find  $h^*$  such that  $\tilde{\phi}_{Y|T^*}^{(a)}(Z; P) - (A - \pi_1)h^*(X)$  is orthogonal to all of  $\mathcal{T}^\perp$ , that is,

$$\forall h: \mathbb{E}_P \left( \left\{ \frac{I(A=a)R}{\mathbb{P}_P(A=a)\mathbb{P}_P(R=1|A=a)} \{Y - \theta_{Y|T^*}^{(a)}(P)\} - (A - \pi_1)h^*(X) \right\} (A - \pi_1)h(X) \right) = 0,$$

from which it follows that

$$\mathbb{E}_P \left( \left\{ \frac{I(A=a)R}{\pi_a \rho_a} \{Y - \theta_{Y|T^*}^{(a)}(P)\} - (A - \pi_1)h^*(X) \right\} (A - \pi_1) \mid X \right) = 0.$$

This implies that

$$\begin{aligned} h^*(X)(1 - \pi_1)\pi_1 &= \mathbb{E}_P \left[ \frac{a - \pi_1}{\pi_a \rho_a} I(A=a)R \{Y - \theta_{Y|T^*}^{(a)}(P)\} \mid X \right] \\ &= \frac{a - \pi_1}{\pi_a \rho_a} \mathbb{E}_P \left[ I(A=a)R \mathbb{E}_P \left\{ Y - \theta_{Y|T^*}^{(a)}(P) \mid A, R, X \right\} \mid X \right] \\ &= \frac{a - \pi_1}{\pi_a \rho_a} \mathbb{P}_P(A=a, R=1 \mid X) \mathbb{E}_P \left\{ Y - \theta_{Y|T^*}^{(a)}(P) \mid A=a, R=1, X \right\} \\ &\stackrel{(A1)}{=} \frac{(a - \pi_1)}{\rho_a} \mathbb{P}_P(R=1 \mid A=a, X) \mathbb{E}_P \left\{ Y - \theta_{Y|T^*}^{(a)}(P) \mid A=a, R=1, X \right\}. \end{aligned}$$

It follows that

$$\begin{aligned} \phi_{Y|T^*}^{(a)}(Z; P) &= \frac{I(R=1)I(A=a)}{\pi_a \rho_a} \{Y - \theta_{Y|T^*}^{(a)}(P)\} \\ &\quad - \frac{(A - \pi_1)(a - \pi_1)}{\rho_a \pi_1 (1 - \pi_1)} \left\{ Q_a(X; P) - \theta_{Y|T^*}^{(a)}(P) \right\} \Pi_a(X; P), \end{aligned} \quad (5)$$

with  $Q_a(X; P) = \mathbb{E}_P\{Y \mid A=a, R=1, X\}$ , and  $\Pi_a(X; P) = \mathbb{P}_P(R=1 \mid A=a, X)$ .

### 3.2 Deriving the Efficient Influence Function for $\theta_{T^*}^{(a)}$

We let the cumulative incidence of cause 1 be defined as

$$F_1(t | a, x) = \mathbb{P}(T^* \leq t, \epsilon^* = 1 | A = a, X = x)$$

and note that the parameter of interest is given by  $\theta_{T^*}^{(a)} = \mathbb{E}[F_1(\tau | a, X)]$  at a prespecified time  $\tau$ . In the full-data case we obtain a tangent space similar to (3) and it follows (see for example (Tsiatis, 2006)) that the EIF is given by

$$\begin{aligned} \phi_{T^*}^{(a),*}(Z^*; P_0) &= \frac{I(A = a)}{\mathbb{P}(A = a)} \{I(T^* \leq \tau, \epsilon^* = 1) - \mathbb{P}(T^* \leq \tau, \epsilon^* = 1 | X, A)\} + \\ &\quad \mathbb{P}(T^* \leq \tau, \epsilon^* = 1 | X, A = 1) - \theta_{Y|T^*}^{(a)}(P_0), \end{aligned} \quad (6)$$

where we let  $Z^* = (T^*, \epsilon^*, A, X)$  denote the full-data, and  $Z = (T, \epsilon, \Delta, A, X)$  denote the observed data. The binary indicator  $I(T^* \leq \tau, \epsilon^* = 1)$  in the above expression cannot be observed due to right-censoring. We let  $\Delta(t) = I(C > T^* \wedge t)$ . Due to the right-censoring we only observe  $\Delta(t)I(T^* < \tau, \epsilon^* = 1)$ , which suggests an inverse probability of censoring weighting (IPCW) correction (Blanche et al., 2023) of the form

$$\phi_{T^*, IPCW}^{(a)}(Z; P_0) = \frac{\Delta(\tau)\phi_{T^*}^{(a),*}(Z^*; P_0)}{G_c(\tau \wedge T | A)} = \frac{\Delta I(T \leq \tau)}{G_c(T | A)} \phi_{T^*}^{(a),*}(Z; P_0) + \frac{I(T > \tau)}{G_c(\tau | A)} \phi_{T^*}^{(a),*}(Z; P_0)$$

where  $G_c(t, a) = \mathbb{P}(C > t | A = a)$ . This IF corresponds to a consistent estimator of the target parameter (1) due to the conditional independent censoring assumption given treatment (A5) and the positivity assumption (A7).

In the following, let  $\lambda_c(t | A)$  denote the hazard rate of the right-censoring process given treatment  $A$ , and let  $M_c(t | A)$  be the censoring martingale, i.e.,

$$M_c(t | A) = 1(T \leq t, \Delta = 0) - \Lambda_c(t | A)$$

where  $\Lambda_c(t | A) = \int_0^t I(T \geq u)\lambda_c(u | A) du$ . It can now be shown (see for example Laan and Robins (2003), and Chapter 10 of Tsiatis (2006)) that the EIF for the observed data  $Z = (T, \Delta, A, X)$  is given by

$$\phi_{T^*}^{(a)}(Z; P_0) = \frac{\Delta(\tau)\phi_{T^*}^{(a),*}(Z; P_0)}{G_c(\tau \wedge T | A)} + \int_0^\tau \frac{\mathbb{E}[\phi_{T^*}^{(a),*}(Z; P_0) | T^* \geq u, A, X]}{G_c(u | A)} dM_c(u | A). \quad (7)$$

In terms of the integrand, we note from (6), that this requires evaluation of the term

$$\mathbb{E}[I(T^* \leq \tau, \epsilon^* = 1) | T^* > u, A, X] = I(u < \tau) \frac{F_1(\tau | A, X) - F_1(u | A, X)}{S(u | A, X)} \quad (8)$$

where  $S(u | A, X) = \mathbb{P}(T > u | A, X)$  is the overall survival probability.

### 3.3 Estimation procedure and asymptotics

We note that for the estimator  $\theta_{Y|T^*}^{(a)} = \mathbb{E}[Y^{(a)} | T^{*(a)} > \tau]$  the influence function,  $\phi_{Y|T^*}^{(a)}(Z; P)$ , defined in (5), evaluated in the true probability distribution of  $Z$  depends only on the probability distribution through  $\mathcal{Q} = \{Q_a(X) = \mathbb{E}[Y | A = a, X, R = 1], \Pi_a(X) = \mathbb{P}(R = 1 | A = a, X), \rho_a = \mathbb{P}(R = 1 | A = a), \pi_a = \mathbb{P}(A = a), \theta_{Y|T^*}^{(a)} | a = 0, 1\}$ . We may construct a *one-step estimator* (Hines et al., 2022) in the following way. Let  $\widehat{\mathcal{Q}} := \{\widehat{Q}_a, \widehat{\Pi}_a, \widehat{\rho}_a, \widehat{\pi}_a, \widehat{\theta}_{Y|T^*}^{(a)} | a = 0, 1\}$  be estimates obtained from the observed data where the estimators for the last two terms can be fully non-parametric and consistently estimated as in (4) and the two first components are obtained as predictions from

some regression models. The initial estimate of  $\theta_{Y|T^*}^{(a)}$  can now be made efficient by adding the debiasing term derived from the plugin estimate of the efficient influence function

$$\widehat{\theta}_{Y|T^*}^{(a)} = \widetilde{\theta}_{Y|T^*}^{(a)} + \mathbb{P}_n \phi_{Y|T^*}^{(a)}(Z; \widehat{\mathcal{Q}})$$

where we use the notation  $\mathbb{P}_n$  to denote the empirical mean over the iid observed data  $Z_1, \dots, Z_n$  but keeping  $\widehat{\mathcal{Q}}$  fixed. The randomization of the treatment  $A$  guarantees that this estimator is consistent irrespectively of how we model the conditional means  $Q_a(X)$  and  $\Pi_a(X)$ . Let  $\widehat{Q}_a(X)$  and  $\widehat{\Pi}_a(X)$  be the two misspecified regression models that converges to  $Q_a^*(X) \neq Q_a(X; P)$  and  $\Pi_a^*(X) \neq \Pi_a(X; P)$  in the sense that  $\mathbb{P} \left\{ (Q_a^*(X) - \widehat{Q}_a(X))^2 \right\}$  and  $\mathbb{P} \left\{ (\Pi_a^*(X) - \widehat{\Pi}_a(X))^2 \right\}$  converges to zero. It follows that the estimating equation derived from the EIF is still consistent

$$\begin{aligned} \mathbb{E}[\phi_{Y|T^*}^{(a)}(Z; \mathcal{Q}^*)] &= 0 - \mathbb{E} \left[ \frac{(A - \pi_1)(a - \pi_1)}{\rho_a \pi_1 (1 - \pi_1)} \{Q_a^*(X) - \theta_{Y|T^*}^{(a)}\} \Pi_a^*(X) \right] \\ &= \mathbb{E} \left\{ \mathbb{E} \left[ \frac{(A - \pi_1)(a - \pi_1)}{\rho_a \pi_1 (1 - \pi_1)} \mid X \right] \{Q_a^*(X) - \theta_{Y|T^*}^{(a)}\} \Pi_a^*(X) \right\} = 0. \end{aligned}$$

where  $\mathcal{Q}^* := \{Q_a^*, \Pi_a^*, \rho_a, \pi_a, \theta_{Y|T^*}^{(a)} \mid a = 0, 1\}$ . We can now decompose the one-step estimator in the following way. Define the remainder term  $R(\widehat{\mathcal{Q}}) = \mathbb{P} \phi_{Y|T^*}^{(a)}(Z; \widehat{\mathcal{Q}}) + \widetilde{\theta}_{Y|T^*}^{(a)} - \theta_{Y|T^*}^{(a)}$ , then direct calculations yield the following von-Mises expansion

$$\begin{aligned} \widehat{\theta}_{Y|T^*}^{(a)} - \theta_{Y|T^*}^{(a)} &= \mathbb{P}_n \phi_{Y|T^*}^{(a)}(Z; \widehat{\mathcal{Q}}) + \widetilde{\theta}_{Y|T^*}^{(a)} - \theta_{Y|T^*}^{(a)} \\ &= (\mathbb{P}_n - \mathbb{P}) \phi_{Y|T^*}^{(a)}(Z; \mathcal{Q}^*) + \\ &\quad (\mathbb{P}_n - \mathbb{P}) \{ \phi_{Y|T^*}^{(a)}(Z; \widehat{\mathcal{Q}}) - \phi_{Y|T^*}^{(a)}(Z; \mathcal{Q}^*) \} + \\ &\quad R(\widehat{\mathcal{Q}}), \end{aligned}$$

where the empirical process term,  $(\mathbb{P}_n - \mathbb{P}) \{ \phi_{Y|T^*}^{(a)}(Z; \widehat{\mathcal{Q}}) - \phi_{Y|T^*}^{(a)}(Z; \mathcal{Q}^*) \}$ , can be controlled to be  $o_P(n^{-1/2})$  even when the nuisance models,  $Q$  and  $\Pi$ , are estimated with machine learning methods, as long as the nuisance models and the corresponding influence function are learned using cross-fitting (Chernozhukov et al., 2018) and we assume that  $\widehat{Q}_a(X)$  and  $Q_a^*(X)$  are bounded almost surely. For the remainder term, we have

$$\begin{aligned} R(\widehat{\mathcal{Q}}) &= \underbrace{\widetilde{\theta}_{Y|T^*}^{(a)} - \theta_{Y|T^*}^{(a)} + \mathbb{P} \left[ \frac{I(A=a)R(Y - \widetilde{\theta}_{Y|T^*}^{(a)})}{\widehat{\pi}_a \widehat{\rho}_a} \right]}_{\mathcal{S}_1} + \\ &\quad \underbrace{\mathbb{P} \left[ \frac{(A - \widehat{\pi}_1)(\widehat{\pi}_1 - a)}{\widehat{\pi}_a \widehat{\rho}_a (1 - \widehat{\pi}_1)} \{ \widehat{Q}_a(X) - \widetilde{\theta}_{Y|T^*}^{(a)} \} \widehat{\Pi}_a(X) \right]}_{\mathcal{S}_2} \end{aligned}$$

and

$$\mathcal{S}_1 = \frac{\pi_a \rho_a - \widehat{\pi}_a \widehat{\rho}_a}{\widehat{\pi}_a \widehat{\rho}_a} \left( \widetilde{\theta}_{Y|T^*}^{(a)} - \theta_{Y|T^*}^{(a)} \right) = o_P(n^{-1/2})$$



since  $(\tilde{\theta}_{Y|T^*}^{(a)} - \theta_{Y|T^*}^{(a)}) = o_P(1)$  and  $(\pi_a \rho_a - \hat{\pi}_a \hat{\rho}_a)(\hat{\pi}_a \hat{\rho}_a)^{-1} = O_P(n^{-1/2})$ . Further,

$$\begin{aligned} \mathcal{S}_2 &= \{\pi_1 - \hat{\pi}_1\} \mathbb{P} \left[ \frac{(\hat{\pi}_1 - a)}{\hat{\rho}_a(1 - \hat{\pi}_1)\hat{\pi}_1} \{\widehat{Q}_a(X) - \tilde{\theta}_{Y|T^*}^{(a)}\} \widehat{\Pi}_a(X) \right] \\ &= \mathbb{P} \left[ \frac{(\pi_1 - a)}{\rho_a(1 - \pi_1)\pi_1} \{Q_a^*(X) - \theta_{Y|T^*}^{(a)}\} \Pi_a^*(X) \right] \frac{1}{n} \sum_{i=1}^n (\pi_1 - A_i) \\ &+ \mathbb{P} \left[ \frac{(\hat{\pi}_1 - a)}{\hat{\rho}_a(1 - \hat{\pi}_1)\hat{\pi}_1} \{\widehat{Q}_a(X) - \tilde{\theta}_{Y|T^*}^{(a)}\} \widehat{\Pi}_a(X) - \right. \\ &\quad \left. \frac{(\pi_1 - a)}{\rho_a(1 - \pi_1)\pi_1} \{Q_a^*(X) - \theta_{Y|T^*}^{(a)}\} \Pi_a^*(X) \right] (\pi_1 - \hat{\pi}_1). \end{aligned}$$

Note that  $\mathbb{P}\{(\pi - \hat{\pi})^2\}^{1/2} = O_P(n^{-1/2})$ . Thus, the last term is  $o_P(n^{-1/2})$  due to convergence and boundedness of the nuisance models and continuity. It follows that

$$\begin{aligned} \sqrt{n}\{\widehat{\theta}_{Y|T^*}^{(a)} - \theta_{Y|T^*}^{(a)}\} &= \frac{1}{\sqrt{n}} \sum_{i=1}^n \phi_{Y|T^*}^{(a)}(Z_i; \mathcal{Q}^*) + \\ &\quad \frac{(\pi_1 - a)}{\rho_a(1 - \pi_1)\pi_1} \mathbb{E}[\{Q_a^*(X) - \theta_{Y|T^*}^{(a)}\} \Pi_a^*(X)] \frac{1}{\sqrt{n}} \sum_{i=1}^n (\pi_1 - A_i) + o_P(1) \\ &= \frac{1}{\sqrt{n}} \sum_{i=1}^n \xi_{Y|T^*}^{(a)}(Z_i; \mathcal{Q}^*) + o_P(1) \end{aligned}$$

and from the CLT that

$$\sqrt{n}\{\widehat{\theta}_{Y|T^*}^{(a)} - \theta_{Y|T^*}^{(a)}\} \rightsquigarrow \mathcal{N}(0, \sigma^2),$$

where the variance estimate  $\sigma^2$  can be consistently estimated from the empirical variance of

$$\xi_{Y|T^*}^{(a)}(Z; \widehat{\mathcal{Q}}) = \phi_{Y|T^*}^{(a)}(Z_i; \widehat{\mathcal{Q}}) + \frac{(\hat{\pi}_1 - a)}{\hat{\rho}_a(1 - \hat{\pi}_1)\hat{\pi}_1} \mathbb{P}_n[\{\widehat{Q}_a(X) - \tilde{\theta}_{Y|T^*}^{(a)}\} \widehat{\Pi}_a(X)](\hat{\pi}_1 - A).$$

The joint distribution of  $(\widehat{\theta}_{Y|T^*}^{(1)}, \widehat{\theta}_{Y|T^*}^{(0)})^\top$  follows directly from stacking the two influence functions

$$\sqrt{n} \left\{ \begin{pmatrix} \widehat{\theta}_{Y|T^*}^{(1)} \\ \widehat{\theta}_{Y|T^*}^{(0)} \end{pmatrix} - \begin{pmatrix} \theta_{Y|T^*}^{(1)} \\ \theta_{Y|T^*}^{(0)} \end{pmatrix} \right\} = \frac{1}{\sqrt{n}} \sum_{i=1}^n \begin{pmatrix} \xi_{Y|T^*}^{(1)}(Z_i; \mathcal{Q}^*) \\ \xi_{Y|T^*}^{(0)}(Z_i; \mathcal{Q}^*) \end{pmatrix} + o_P(1),$$

which converges weakly to a Gaussian with asymptotic variance that can be approximated by

$$\widehat{\Sigma} = \frac{1}{n} \sum_{i=1}^n \begin{pmatrix} \xi_{Y|T^*}^{(1)}(Z_i; \widehat{\mathcal{Q}})^2 & \xi_{Y|T^*}^{(0)}(Z_i; \widehat{\mathcal{Q}}) \xi_{Y|T^*}^{(1)}(Z_i; \widehat{\mathcal{Q}}) \\ \xi_{Y|T^*}^{(0)}(Z_i; \widehat{\mathcal{Q}}) \xi_{Y|T^*}^{(1)}(Z_i; \widehat{\mathcal{Q}}) & \xi_{Y|T^*}^{(0)}(Z_i; \widehat{\mathcal{Q}})^2 \end{pmatrix}.$$

Finally, the estimate for  $\psi_{Y|T^*} = \theta_{Y|T^*}^{(1)} - \theta_{Y|T^*}^{(0)}$ , is obtained as

$$\widehat{\psi}_{Y|T^*} = \widehat{\theta}_{Y|T^*}^{(1)} - \widehat{\theta}_{Y|T^*}^{(0)}$$

with the asymptotic variance approximated by  $(1 - 1)\widehat{\Sigma}(1 - 1)^\top$  and estimated influence function given by

$$\xi_{Y|T^*}^{(1)}(Z_i; \widehat{\mathcal{Q}}) - \xi_{Y|T^*}^{(0)}(Z_i; \widehat{\mathcal{Q}}).$$

Similarly, a semi-parametric efficient estimate of  $\theta_{T^*}^{(a)}$  can be obtained from the EIF (7), and combined in a similar fashion into an estimate,  $\widehat{\psi}_{T^*}$  of the target parameter  $\psi_{T^*} = \theta_{T^*}^{(0)} - \theta_{T^*}^{(1)}$ .

The details of this estimation procedure are given in more details in (Blanche et al., 2023) and are implemented in the R function `rets::binregATE` (Holst and Scheike, 2024). With access to the EIFs for both  $\widehat{\psi}_{T^*}$  and  $\widehat{\psi}_{Y|T^*}$  we can use the stacking method above to calculate the joint asymptotic distribution and correlation between the estimates that we need for applying the multiple testing procedure that we describe in details in the next section. The estimator is implemented in the targeted R package (Holst and Nordland, 2024) and implementation details are given in the Appendix.

## 4 A closed testing procedure based on signed Wald tests

In order to provide family-wise error control at  $\alpha$  level when simultaneously evaluating  $H_{Y|T^*}$  and  $H_{T^*}$  we propose a closed testing procedure in which  $H_{Y|T^*} \cap H_{T^*}$  is evaluated with an  $\alpha$  level test and, contingent on the rejection of the intersection hypothesis,  $H_{Y|T^*}$  and  $H_{T^*}$  are evaluated separately, also by  $\alpha$  level tests (Marcus et al., 1976).

### 4.1 Theoretical properties

To efficiently test the intersection hypothesis at  $\alpha$  level we consider a Wald test proposed in for instance (Robertson et al., 1988, p. 224) or (Silvapulle, 1992) for general-purpose hypothesis testing. In our particular context, we consider a version of this test that is truncated at zero for values below zero, and we term this the signed Wald test in what follows. Accordingly, the signed Wald test for testing  $H_{Y|T^*} \cap H_{T^*}$  is defined as follows:

$$SW_{n, H_{Y|T^*} \cap H_{T^*}} = \inf_{\psi \in H_{Y|T^*} \cap H_{T^*}} \{n \cdot \{\widehat{\psi} - \psi\}^\top \widehat{\Sigma}^{-1} \{\widehat{\psi} - \psi\}\},$$

where  $\psi = \{\psi_{Y|T^*}, \psi_{T^*}\}^T$  and  $\widehat{\psi} = \{\widehat{\psi}_{Y|T^*}, \widehat{\psi}_{T^*}\}^T$ .

In order to derive large sample properties of  $SW_{n, H_1 \cap H_2}$  we first rewrite above expression in terms of  $\widehat{u} = \sqrt{n} \cdot \sqrt{\widehat{\Sigma}}^{-1} \{\widehat{\psi} - (\delta_{Y|T^*}, -\delta_{T^*})^\top\}$  and  $u = \sqrt{n} \cdot \sqrt{\Sigma}^{-1} \{\psi - (\delta_{Y|T^*}, -\delta_{T^*})^\top\}$  to obtain:

$$SW_{n, H_{Y|T^*} \cap H_{T^*}} = \inf_{\sqrt{\widehat{\Sigma}}u \leq 0} \{\{\widehat{u} - u\}^\top \{\widehat{u} - u\}\} = \inf_{\sqrt{\widehat{\Sigma}}u \leq 0} \|\widehat{u} - u\|^2 \quad (9)$$

As illustrated in Figure 1 the region  $\{u : \sqrt{\widehat{\Sigma}}u \leq 0\}$  is enclosed by the two lines  $\widehat{L}_1$  and  $\widehat{L}_2$ . Note that if  $\widehat{u}$  belongs to that region the signed wald test equals zero. If  $\widehat{u} \in \widehat{A}_1$  we know that the projection of  $\widehat{u}$  onto  $\widehat{L}_1$  is the point in  $\{u : \sqrt{\widehat{\Sigma}}u \leq 0\}$  closest to  $\widehat{u}$ . Accordingly, for  $\widehat{u} \in \widehat{A}_1$ , we have  $SW_{n, H_1 \cap H_2} = \|\widehat{u} - P_{\widehat{L}_1}(\widehat{u})\|^2$ , where  $P_{\widehat{L}_1}(\widehat{u})$  denotes the projection of  $\widehat{u}$  onto  $\widehat{L}_1$ . Similarly it follows that  $SW_{n, H_1 \cap H_2} = \|\widehat{u} - P_{\widehat{L}_2}(\widehat{u})\|^2$  for  $\widehat{u} \in \widehat{A}_3$ . Finally, for  $\widehat{u} \in \widehat{A}_2$  the point in  $\{u : \sqrt{\widehat{\Sigma}}u \leq 0\}$  closest to  $\widehat{u}$  is zero and accordingly  $SW_{n, H_1 \cap H_2} = \|\widehat{u}\|^2$  in this case.

In summary, we conclude that the signed Wald test for  $H_{Y|T^*} \cap H_{T^*}$  may be rewritten as:

$$SW_{n, H_{Y|T^*} \cap H_{T^*}} = I(\widehat{u} \in \widehat{A}_1) \cdot \|\widehat{u} - P_{\widehat{L}_1}(\widehat{u})\|^2 + I(\widehat{u} \in \widehat{A}_3) \cdot \|\widehat{u} - P_{\widehat{L}_2}(\widehat{u})\|^2 + I(\widehat{u} \in \widehat{A}_2) \cdot \|\widehat{u}\|^2$$

Next note that when  $\psi = (\delta_{Y|T^*}, -\delta_{T^*})^\top$  we have that  $\widehat{u}$  converges weakly to a zero mean standard normal distribution. We also have that  $\widehat{\Sigma}$  converges in probability to some positive definite matrix  $\Sigma$ . It follows from the above representation of  $SW_{n, H_{Y|T^*} \cap H_{T^*}}$  that for  $\psi = (\delta_{Y|T^*}, -\delta_{T^*})^\top$ :

$$SW_{n, H_{Y|T^*} \cap H_{T^*}} \rightsquigarrow \left(\frac{1}{2} - q\right) \cdot \chi_0^2 + \frac{1}{2} \cdot \chi_1^2 + q \cdot \chi_2^2 \quad (10)$$

where

$$q = P(\varepsilon \in A_2)$$

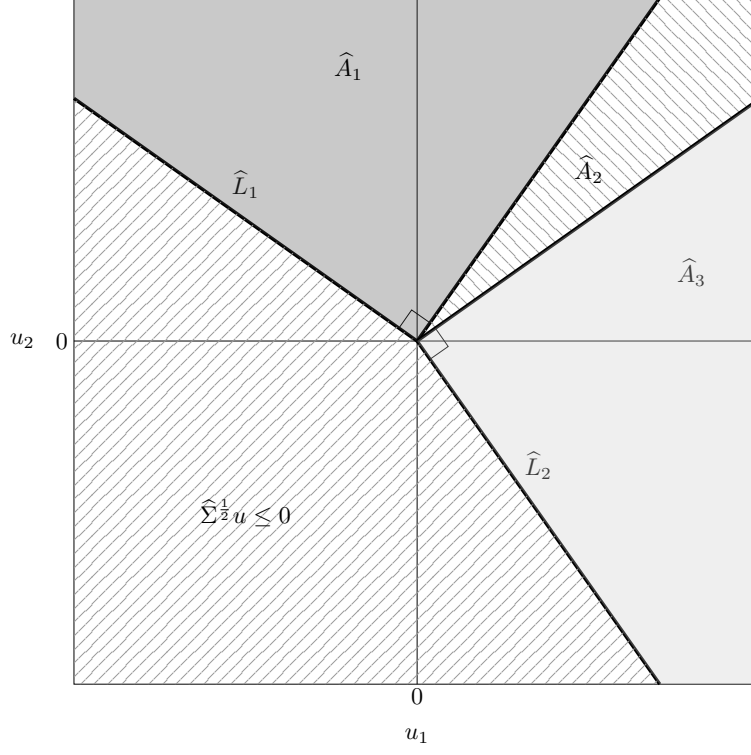


Figure 1: Regions characterizing the value of the signed Wald test

with  $\varepsilon \sim N(0, I_{2 \times 2})$  and  $A_2$  defined as  $\hat{A}_2$  when replacing  $\hat{\Sigma}$  by  $\Sigma$ . It follows that the p-value, that is the maximal tail probability in the distribution of  $SW_{n, H_Y|T^* \cap H_{T^*}}$  under the null hypothesis, can be approximated as

$$\begin{aligned} \sup_{\psi \in H_Y|T^* \cap H_{T^*}} P_{\psi}(SW_{n, H_Y|T^* \cap H_{T^*}} \geq x) &= P_{\psi=(\delta_{Y|T^*}, -\delta_{T^*})^\top}(SW_{n, H_Y|T^* \cap H_{T^*}} \geq x) \\ &\longrightarrow P(SW_{H_Y|T^* \cap H_{T^*}} \geq x), \text{ as } n \rightarrow \infty \end{aligned}$$

where

$$SW_{H_Y|T^* \cap H_{T^*}} \sim \left(\frac{1}{2} - q\right) \cdot \chi_0^2 + \frac{1}{2} \cdot \chi_1^2 + q \cdot \chi_2^2.$$

To calculate the p-value in practice based on the above approximation we also need to consistently estimate  $q$  and plug the resulting estimator into the righthand side of (10). Such an estimator is obtained by noting that:

$$P(\sqrt{\Sigma}\varepsilon \leq 0) = \frac{1}{2} - q.$$

It follows that we can consistently estimate  $q$  by:

$$\hat{q} = \frac{1}{2} - P(\sqrt{\hat{\Sigma}}\varepsilon \leq 0).$$

Here we note that  $P(\sqrt{\hat{\Sigma}}\varepsilon \leq 0)$  is easy to calculate by either simulation or numerical integration.

Also in order to more easily calculate  $SW_{n, H_Y|T^* \cap H_{T^*}}$  in practice we re-express this quantity in terms of the standardized estimates  $z_{Y|T^*} = \frac{\sqrt{n} \cdot (\hat{\psi}_{Y|T^*} - \delta_{Y|T^*})}{\sqrt{\hat{\Sigma}_{11}}}$ ,  $z_{T^*} = \frac{\sqrt{n} \cdot (\hat{\psi}_{T^*} + \delta_{T^*})}{\sqrt{\hat{\Sigma}_{22}}}$ , and the estimated correlation  $\hat{\rho} = \frac{\hat{\Sigma}_{12}}{\sqrt{\hat{\Sigma}_{11} \cdot \hat{\Sigma}_{22}}}$  between the estimators. By brute force calculation we obtain:

$$\begin{aligned}
SW_{n, H_{Y|T^*} \cap H_{T^*}} &= I(z_{Y|T^*} \geq 0, z_{T^*} \leq \hat{\rho} \cdot z_{Y|T^*}) \cdot z_{Y|T^*}^2 + I(z_{T^*} \geq 0, z_{Y|T^*} \leq \hat{\rho} \cdot z_{T^*}) \cdot z_{T^*}^2 \\
&+ I(z_{Y|T^*} \geq 0, z_{T^*} \geq \hat{\rho} \cdot z_{Y|T^*} \cup z_{T^*} \geq 0, z_{Y|T^*} \geq \hat{\rho} \cdot z_{T^*}) \frac{z_{Y|T^*}^2 + z_{T^*}^2 - 2 \cdot \hat{\rho} \cdot z_{Y|T^*} \cdot z_{T^*}}{1 - \hat{\rho}^2}
\end{aligned}$$

which is straightforward to calculate by plug in.

We shall also subsequently use that  $SW_{n, H_{Y|T^*} \cap H_{T^*}}$  can be represented in terms of  $z_{min} = \min\{z_{Y|T^*}, z_{T^*}\}$  and  $z_{max} = \max\{z_{Y|T^*}, z_{T^*}\}$  as:

$$\begin{aligned}
SW_{n, H_{Y|T^*} \cap H_{T^*}} &= I(z_{max} \geq 0, z_{min} \leq \hat{\rho} \cdot z_{max}) \cdot z_{max}^2 + \\
&+ I(z_{max} \geq 0, z_{min} \geq \hat{\rho} \cdot z_{max}) \frac{(z_{max} - z_{min})^2 + 2 \cdot (1 - \hat{\rho}) \cdot z_{min} \cdot z_{max}}{1 - \hat{\rho}^2} \quad (11)
\end{aligned}$$

For testing the single hypotheses  $H_{Y|T^*}$  and  $H_{T^*}$  we again use signed Wald tests which are the standard testing tool for single parameter superiority/non-inferiority testing. Specifically, the single hypothesis signed Wald tests are given by:

$$\begin{aligned}
SW_{n, H_{Y|T^*}} &= I(z_{Y|T^*} \geq 0) \cdot z_{Y|T^*}^2, \\
SW_{n, H_{T^*}} &= I(z_{T^*} \geq 0) \cdot z_{T^*}^2.
\end{aligned}$$

The accompanying p-values are computed by approximations similar to that of the intersection hypothesis test, that is:

$$\begin{aligned}
\sup_{\psi \in H_{Y|T^*}} P_\psi(SW_{n, H_{Y|T^*}} \geq x) &= P_{\psi_{Y|T^*} = \delta_{Y|T^*}}(SW_{n, H_{Y|T^*}} \geq x) \rightarrow P(SW_{H_{Y|T^*}} \geq x), \text{ as } n \rightarrow \infty, \\
\sup_{\psi \in H_{T^*}} P_\psi(SW_{n, H_{T^*}} \geq x) &= P_{\psi_{T^*} = -\delta_{T^*}}(SW_{n, H_{T^*}} \geq x) \rightarrow P(SW_{H_{T^*}} \geq x), \text{ as } n \rightarrow \infty,
\end{aligned}$$

where

$$\begin{aligned}
SW_{H_{Y|T^*}} &\sim \frac{1}{2} \cdot \chi_0^2 + \frac{1}{2} \cdot \chi_1^2, \\
SW_{H_{T^*}} &\sim \frac{1}{2} \cdot \chi_0^2 + \frac{1}{2} \cdot \chi_1^2.
\end{aligned}$$

## 4.2 Some general power considerations

We now give some insights to the rejection regions of the proposed testing procedure for rejecting at least one of the hypotheses  $H_{Y|T^*}$  and  $H_{T^*}$  as well as for rejecting both hypotheses. We next use these insights to argue that in scenarios with substantial positive correlation between the estimated target parameters our proposal will have higher disjunctive (win on at least one) power than the Bonferroni-Holm procedure under any alternative. Moreover we argue that our proposal will have higher conjunctive (win on all) power than the Bonferroni-Holm procedure in all correlation scenarios and under all alternatives. In the below derivations we fix  $\alpha$  at 2.5%. Consequently all derived thresholds and critical values are specific to this value. However, all derivations are easily repeated for any other choice of  $\alpha$ .

As first step we evaluate the critical values of the intersection signed Wald test  $SW_{n, H_{Y|T^*} \cap H_{T^*}}$  as a function of the estimated correlation  $\hat{\rho}$  between the estimators. This can be done by numerically calculating  $\hat{q}$  for each value of the correlation and then follow the steps described above with a fixed significance level  $\alpha$ . The resulting critical values are shown in Figure 2.

From a numerical search we find that for a correlation of 0.57 the critical value of  $SW_{n, H_{Y|T^*} \cap H_{T^*}}$  equals the  $1 - \alpha/2$  quantile in the  $\frac{1}{2}\chi_0^2 + \frac{1}{2}\chi_1^2$  distribution. We denote this quantile by  $(\frac{1}{2}\chi_0^2 +$

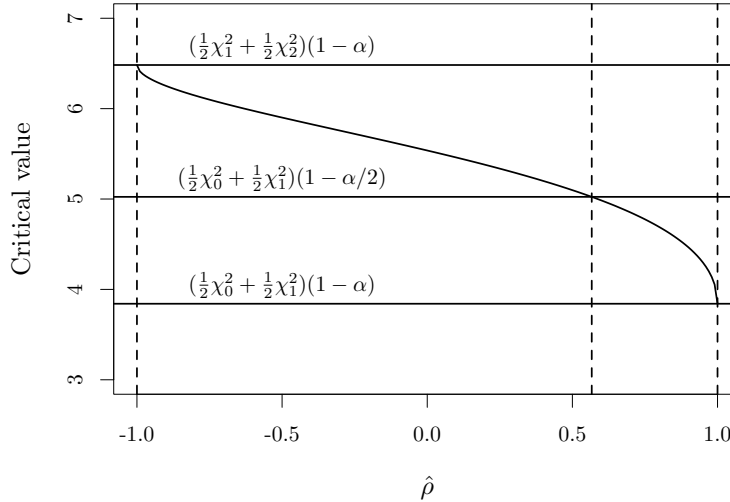


Figure 2: Critical values of  $SW_{n, H_{Y|T^*} \cap H_{T^*}}$  as a function of correlation between estimators for  $\alpha = 0.025$ . The solid lines mark the  $1 - \alpha$ ,  $1 - \alpha/2$ , and  $1 - \alpha$  quantiles in the  $\frac{1}{2}\chi_1^2 + \frac{1}{2}\chi_2^2$ ,  $\frac{1}{2}\chi_0^2 + \frac{1}{2}\chi_1^2$ , and  $\frac{1}{2}\chi_0^2 + \frac{1}{2}\chi_1^2$ , respectively. Dashed lines mark the correlations where the critical values of  $SW_{n, H_{Y|T^*} \cap H_{T^*}}$  equal these quantiles

$\frac{1}{2}\chi_1^2)(1 - \alpha/2)$  in what follows. Since the critical values of  $SW_{n, H_{Y|T^*} \cap H_{T^*}}$  are decreasing as a function of correlation we note that for correlations above 0.57 the critical values of  $SW_{n, H_{Y|T^*} \cap H_{T^*}}$  are below  $(\frac{1}{2}\chi_0^2 + \frac{1}{2}\chi_1^2)(1 - \alpha/2)$ .

In order to reject at least one of the hypotheses  $H_{Y|T^*}$  or  $H_{T^*}$  with the Bonferroni-Holm procedure it is required that  $I(z_{max} \geq 0)z_{max}^2 = \max\{SW_{n, H_{Y|T^*}}, SW_{n, H_{T^*}}\} \geq (\frac{1}{2}\chi_0^2 + \frac{1}{2}\chi_1^2)(1 - \alpha/2)$ . It further follows from the representation (11) and some straightforward calculations that  $SW_{n, H_{Y|T^*} \cap H_{T^*}} \geq I(z_{max} \geq 0)z_{max}^2$ . This means that for a correlation above 0.57 we reject  $SW_{n, H_{Y|T^*} \cap H_{T^*}}$  when we reject at least one hypothesis with the Bonferroni-Holm procedure. In this case we also reject at least one hypothesis with our proposal since  $SW_{n, H_{Y|T^*} \cap H_{T^*}}$  is rejected and  $SW_{n, H_{Y|T^*}}$  or  $SW_{n, H_{T^*}}$  exceeds the  $1 - \alpha/2$  quantile and therefore also the  $1 - \alpha$  quantile in the  $\frac{1}{2}\chi_0^2 + \frac{1}{2}\chi_1^2$  distribution.

In summary, the above considerations show that for a correlation above 0.57 a higher disjunctive power is ensured with our proposal compared to the Bonferroni-Holm procedure.

Next, we turn to the conjunctive power, that is, the probability of rejecting both hypotheses. We first note that in order for the Bonferroni-Holm procedure to reject both hypotheses it is required that  $I(z_{max} \geq 0)z_{max}^2 > (\frac{1}{2}\chi_0^2 + \frac{1}{2}\chi_1^2)(1 - \alpha/2)$  and  $I(z_{min} \geq 0)z_{min}^2 > (\frac{1}{2}\chi_0^2 + \frac{1}{2}\chi_1^2)(1 - \alpha)$ .

To proceed we now view  $SW_{n, H_{Y|T^*} \cap H_{T^*}}$  as a function of  $z_{min}$  and  $z_{max}$  for fixed  $\rho$  according to (11). In Figure 3 we plotted the level curves of  $SW_{n, H_{Y|T^*} \cap H_{T^*}}$  as a function of positive values of  $z_{min}$  and  $z_{max}$  for a range of fixed  $\hat{\rho}$ s. Since  $SW_{n, H_{Y|T^*} \cap H_{T^*}}$  is increasing on any line segment it is clear from Figure 3 that any point in the conjunctive rejection region of the Bonferroni-Holm procedure is also rejected by the proposed procedure irrespective of the value of  $\hat{\rho}$ .

To further gauge the actual power gain we calculate the conjunctive power of the proposed test strategy under a given alternative when testing using superiority/non-inferiority margins  $\delta_{Y|T^*} = \delta_{T^*} = 0$  in  $H_{T^*}$  and with  $\alpha = 0.025$ . For each value of the correlation  $\hat{\rho}$ , the alternative is chosen to yield a non centrality parameter  $(r(\hat{\rho}), r(\hat{\rho})) > 0$  of  $(z_{Y|T^*}, z_{T^*})$  that will result in a conjunctive power of 80% for the Bonferroni-Holm procedure. For each value of the correlation we

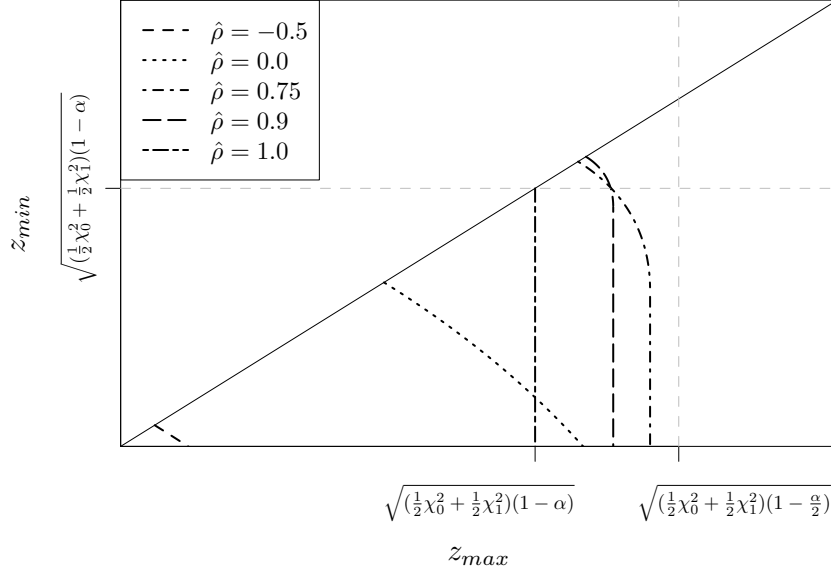


Figure 3: Dashed lines show the level curves of  $SW_{n, H_Y|T^* \cap H_{T^*}}$  at the critical value ( $\alpha = 2.5\%$ ) for positive values of  $z_{min}$  and  $z_{max}$  and a range of correlations  $\hat{\rho}$ .

calculate the conjunctive power of the proposed strategy by simulating 10 million realisations of  $(z_{Y|T^*}, z_{T^*})$  with the given non-centrality parameter and for each realization we then determine the outcome of the test strategy. Resulting conjunctive powers are plotted in Figure 4 below as a function of the correlation.

Similarly we calculate the disjunctive power in a scenario with non-centrality parameter  $(r(\hat{\rho}), r(\hat{\rho})) > 0$  chosen so that the disjunctive power of the Bonferroni-Holm procedure equals 80%. Resulting disjunctive powers are plotted in Figure 5.

## 5 Simulation study

In order to rigorously assess the performance of our proposed estimators and closed-testing framework in a realistic context, we have designed a comprehensive Monte Carlo simulation study. This simulation has been calibrated to mirror the characteristics of the FLOW trial (Perkovic et al., 2024) to which we also apply the methodology later. The following variables are considered in this simulation study

$T$ : time of first event in years (first major irreversible kidney event or non-related death).

$\epsilon$ : event type at  $T$ ; first major irreversible kidney event ( $\epsilon = 1$ ), non-related death. ( $\epsilon = 2$ ), or right censoring ( $\epsilon = 0$ ).

$Y := Y(\tau)$ : clinical outcome measurement (eGFR) at landmark time  $\tau$ .

$R$ : missing indicator for  $Y$  (1 if observed, 0 if either  $T < \tau$  or if  $Y$  was not measured for other reasons).

$A$ : binary treatment (1: active, 0: placebo).

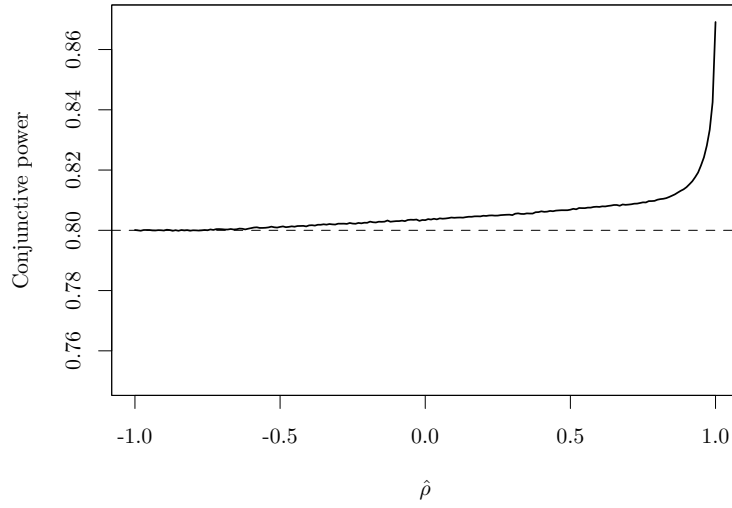


Figure 4: Conjunctive power as a function of  $\hat{\rho}$ . Solid line corresponds to the proposed testing procedure, dashed line corresponds to the Bonferroni-Holm procedure.

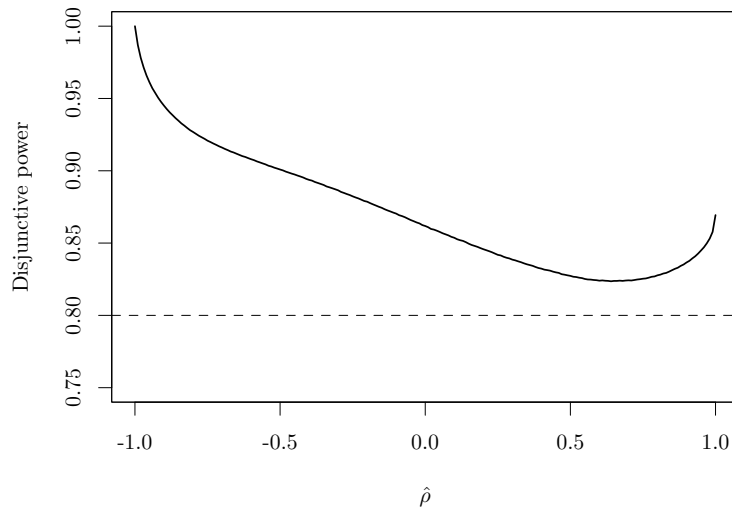


Figure 5: Disjunctive power as a function of  $\hat{\rho}$ . Solid line corresponds to the proposed testing procedure, dashed line corresponds to the Bonferroni-Holm procedure.

$X_1$ : covariate, clinical outcome at baseline (eGFR).

$X_2$ : covariate, binary treatment usage indicator (1: SGLT2 treatment, 0: none).

and let the covariates be distributed according to  $A \sim \text{Bernoulli}(\pi)$ ,  $X_2 \sim \text{Bernoulli}(p_{X_2})$ , and  $X_1 | X_2 = x \sim \mathcal{N}(\mu_x, \sigma_x^2)$ ,  $x \in \{0, 1\}$ . The clinical outcome is modelled as

$$Y | A, X_1, X_2 \sim \mathcal{N}(\beta_{Y,0}^{(A)} + \beta_{Y,1}^{(A)}(X_1 - \mu_1) + \beta_{Y,2}^{(A)}X_2, \sigma_Y^{(A)2}),$$

which is observed conditional on the patients staying in study until the landmark time  $\tau$ , with the missing data mechanism described by ( $R = 1$  actually observed)

$$R | T^* > \tau, A, X_1, X_2 \sim \text{Bernoulli} \left( \text{expit} \{ \beta_{R,0}^{(A)} + \beta_{R,1}^{(A)}(X_1 - \mu_1) + \beta_{R,2}^{(A)}X_2 \} \right)$$

The cause-specific hazard for all events and censoring are modelled as Cox proportional hazard models with the baseline hazard function described by a Weibull hazard function parametrized in the following way

$$\lambda_{\epsilon=k}(t | A, X_1, X_2) = \gamma_{\epsilon=k}^{(A)} t^{\gamma_{\epsilon=k}^{(A)} - 1} \exp \left\{ \beta_{\epsilon=k,0}^{(A)} + \beta_{\epsilon=k,1}^{(A)}(X_1 - \mu_1) + \beta_{\epsilon=k,2}^{(A)}X_2 \right\}, k = 0, 1, 2.$$

## 5.1 Simulation results

The parameters of the simulation study are calibrated to the FLOW study and are defined in Table 1. For the clinical outcome model we observe strong effects of both  $X_1$ , and  $X_2$ . For the cause-specific hazards for both the primary outcome and the competing risk of death from other causes more modest statistical evidence of associations are seen. The censoring distribution is almost entirely driven by administrative censoring and as a natural consequence we do not see any statistical evidence of effects of the two covariates. The same applies for the missing data mechanism conditioned on  $T > \tau$  indicating that the assumptions (A4), (A5) are reasonable in this application and accordingly we enforce these assumptions in the simulation scenarios (Table 1). We consider the fixed landmark time  $\tau = 2$

In Table 2 we present the results of 20,000 simulations from the above setting with a sample size of  $n = 500$ ,  $n = 1,000$ ,  $n = 2,000$ , and  $n = 4,000$  subjects. We estimate in each simulation the parameters

$$\begin{aligned} \psi_{T^*} &= \theta_{T^*}^{(0)} - \theta_{T^*}^{(1)} = \mathbb{P}(T^{*(0)} \leq \tau, \epsilon^{*(0)} = 1) - \mathbb{P}(T^{*(1)} \leq \tau, \epsilon^{*(1)} = 1) \\ \psi_{Y|T^*} &= \theta_{Y|T^*}^{(1)} - \theta_{Y|T^*}^{(0)} = \mathbb{E}[Y^{(1)} | T^{*(1)} > \tau] - \mathbb{E}[Y^{(0)} | T^{*(0)} > \tau] \end{aligned}$$

based on the estimator  $\tilde{\psi}_{Y|T^*}$  that ignores baseline covariate information (4), and the one-step estimator,  $\hat{\psi}_{Y|T^*}$ , derived from the efficient influence function (5). The nuisance models for  $\mathbb{E}(Y | A, R = 1, X_1, X_2)$ ,  $\mathbb{P}(R = 1 | A, X_1, X_2)$  are based on a linear model and logistic model, respectively, with main effects of  $X_1$  and  $X_2$  and stratified by treatment.

Similarly, Aalen-Johansen estimators are used to obtain an initial estimator  $\tilde{\psi}_{T^*}$  of the risk-difference. Subsequently, the efficient one-step estimator  $\hat{\psi}_{T^*}$  is derived based on the EIF (7), where the nuisance model for the cause specific hazards is a Cox regression with main effects  $X_1$  and  $X_2$  and baseline hazard stratified by treatment. The censoring distribution is estimated using a Kaplan-Meier estimate separately in each treatment arm.

The true parameter values are calculated numerically by Monte Carlo integration from a large ( $n = 10^8$ ) simulated data set without censoring or missing data. Resulting values were  $\psi_{Y|T^*} = 2.7896$  and  $\psi_{T^*} = 0.0241$ .

From Table 2 we confirm the consistency of both estimators and the estimates of the asymptotic variance obtained from the variance of the respective influence functions reflected in the nice agreement between the empirical average of the estimated standard errors (SE) and the standard deviation of the parameter estimates over the 20,000 simulation iterations (SD), as well as the



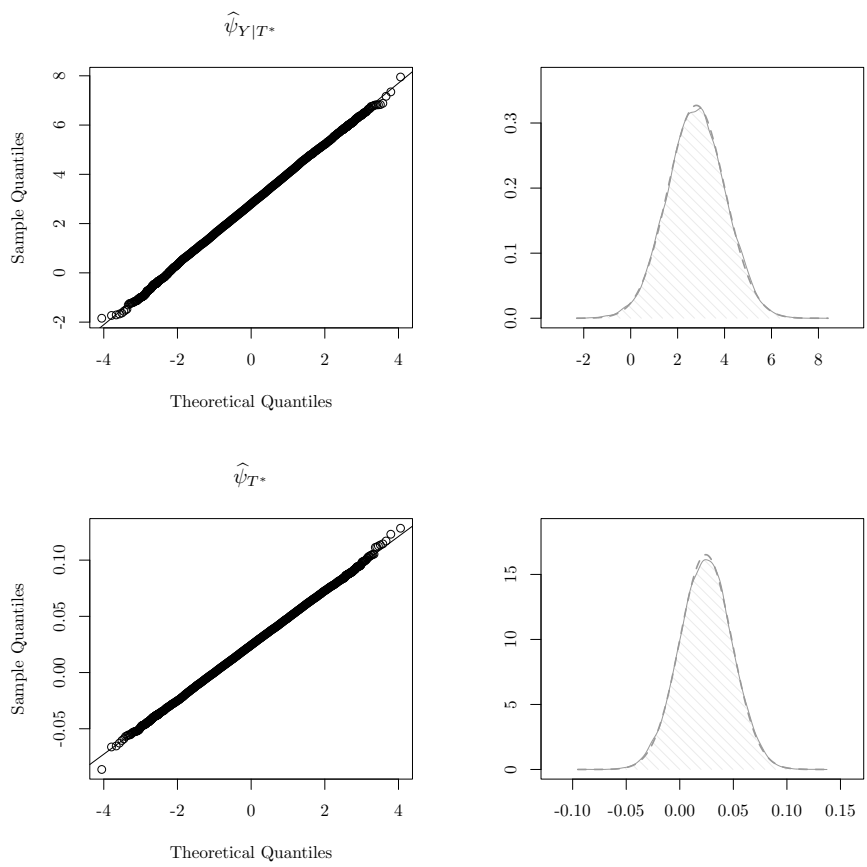


Figure 6: Normal approximation of the simulation study of the parameter estimates at  $n = 500$ .

Table 1: Parameters of the simulation study.

$\pi$								
$A$	0.5							
	$\mu_1$	$\sigma_1$	$\mu_2$	$\sigma_2$				
$X_1$	46.24	14.99	51.15	15.33				
	$\rho_{X_2}$							
$X_2$	0.156							
	$\beta_{Y,0}^{(A=0)}$	$\beta_{Y,1}^{(A=0)}$	$\beta_{Y,2}^{(A=0)}$	$\sigma_Y^{(A=0)}$	$\beta_{Y,0}^{(A=1)}$	$\beta_{Y,1}^{(A=1)}$	$\beta_{Y,2}^{(A=1)}$	$\sigma_Y^{(A=1)}$
$Y$	40.141	0.895	1.993	11.85	43.121	0.863	2.620	12.16
	$\beta_{R,0}^{(A=0)}$	$\beta_{R,1}^{(A=0)}$	$\beta_{R,2}^{(A=0)}$		$\beta_{R,0}^{(A=1)}$	$\beta_{R,1}^{(A=1)}$	$\beta_{R,2}^{(A=1)}$	
$R   T > \tau$	2.243	0	0		2.309	0	0	
	$\beta_{\epsilon=0,0}^{(A=0)}$	$\beta_{\epsilon=0,1}^{(A=0)}$	$\beta_{\epsilon=0,2}^{(A=0)}$	$\gamma_{\epsilon=0}^{(A=0)}$	$\beta_{\epsilon=0,0}^{(A=1)}$	$\beta_{\epsilon=0,1}^{(A=1)}$	$\beta_{\epsilon=0,2}^{(A=1)}$	$\gamma_{\epsilon=0}^{(A=1)}$
$\epsilon = 0$	-8.874	0	0	6.691	-9.278	0	0	6.946
	$\beta_{\epsilon=1,0}^{(A=0)}$	$\beta_{\epsilon=1,1}^{(A=0)}$	$\beta_{\epsilon=1,2}^{(A=0)}$	$\gamma_{\epsilon=1}^{(A=0)}$	$\beta_{\epsilon=1,0}^{(A=1)}$	$\beta_{\epsilon=1,1}^{(A=1)}$	$\beta_{\epsilon=1,2}^{(A=1)}$	$\gamma_{\epsilon=1}^{(A=1)}$
$\epsilon = 1$	-3.558	-0.0243	-0.583	1.822	-4.008	-0.0289	-0.126	1.901
	$\beta_{\epsilon=2,0}^{(A=0)}$	$\beta_{\epsilon=2,1}^{(A=0)}$	$\beta_{\epsilon=2,2}^{(A=0)}$	$\gamma_{\epsilon=2}^{(A=0)}$	$\beta_{\epsilon=2,0}^{(A=1)}$	$\beta_{\epsilon=2,1}^{(A=1)}$	$\beta_{\epsilon=2,2}^{(A=1)}$	$\gamma_{\epsilon=2}^{(A=1)}$
$\epsilon = 2$	-4.173	-0.0205	-0.455	1.143	-4.135	0.00687	-0.598	1.071

estimated coverage of the 95% Wald confidence limits. The Gaussian approximation is excellent already at  $n = 500$  (see Figure 6). Furthermore, as expected the one-step estimator based on the efficient influence function is here considerably more efficient for the parameter  $\psi_{Y|T^*}$  (around 40% larger standard errors in the unadjusted estimator), whereas the efficiency gains are minor for  $\psi_{T^*}$  (around 0.6% larger variance in the unadjusted estimator) due to the weaker association between the covariates  $X_1, X_2$  and the time-to-event outcomes in this simulation.

We next employ the proposed closed testing procedure as well as the Bonferroni-Holm procedure to each simulated data set to assess their performance in terms of power. Results are summarized in Table 3.

From Table 3 we note a substantial power gain when comparing our proposed testing procedure based on the one-step estimators to the traditional Bonferroni-Holm procedure based on the unadjusted estimators. In particular, a substantial power gain is obtained by using the one-step estimators over the unadjusted estimators. A smaller but still appreciable gain in power is seen from using the proposed testing strategy instead of the Bonferroni-Holm procedure.

To assess also type 1 error of the proposed testing procedure under the global null hypothesis  $H_{Y|T^*} \cap H_{T^*}$  we consider a simulation scenario where data in the active treatment arm ( $A = 1$ ) are generated according to the specification for the placebo arm ( $A = 0$ ) in Table 1. Again we simulate 20000 data sets and summarize the performance of our proposed estimation and testing strategy in terms of type 1 error control in Table 4.

From Table 4 we conclude that the type 1 error is controlled well at the nominal 2.5% significance level in all scenarios and when testing both  $H_{Y|T^*} \cap H_{T^*}$ ,  $H_{Y|T^*}$ , and  $H_{T^*}$ .

To finally explore the performance in a situation where there is a stronger association between covariates and the terminal event of interest, we consider a scenario with  $n = 2000$  identical to the parameters in Table 1 except that for the cause-specific hazard for the primary event,  $\epsilon = 1$ , we increase the effect of the covariate  $X_1$  to  $\beta_{\epsilon=1,1}^{(A=1)} = \beta_{\epsilon=1,1}^{(A=0)} = -0.15$ . The summarized results

Table 2: Simulation results based on 20,000 replications in the scenario with parameters defined in Table 1.

$n = 500$							
	Mean	Bias	SE	SD	SE/SD	Coverage	Rel.eff
Naive ( $\tilde{\psi}_{Y T^*}$ )	2.8093	0.0196	1.7020	1.7049	0.9983	0.9475	1.3891
Adjusted/debiased ( $\hat{\psi}_{Y T^*}$ )	2.7987	0.0091	1.2198	1.2273	0.9939	0.9493	1.0000
Naive ( $\tilde{\psi}_{T^*}$ )	0.0244	0.0003	0.0244	0.0245	0.9971	0.9488	1.0056
Adjusted/debiased ( $\hat{\psi}_{T^*}$ )	0.0243	0.0002	0.0242	0.0243	0.9931	0.9475	1.0000
$n = 1,000$							
	Mean	Bias	SE	SD	SE/SD	Coverage	Rel.eff
Naive ( $\tilde{\psi}_{Y T^*}$ )	2.7919	0.0022	1.2046	1.2030	1.0013	0.9502	1.3819
Adjusted/debiased ( $\hat{\psi}_{Y T^*}$ )	2.7814	-0.0082	0.8643	0.8705	0.9929	0.9490	1.0000
Naive ( $\tilde{\psi}_{T^*}$ )	0.0241	0.0000	0.0173	0.0173	0.9971	0.9513	1.0055
Adjusted/debiased ( $\hat{\psi}_{T^*}$ )	0.0240	-0.0001	0.0171	0.0172	0.9940	0.9516	1.0000
$n = 2,000$							
	Mean	Bias	SE	SD	SE/SD	Coverage	Rel.eff
Naive ( $\tilde{\psi}_{Y T^*}$ )	2.7761	-0.0136	0.8521	0.8581	0.9929	0.9473	1.3996
Adjusted/debiased ( $\hat{\psi}_{Y T^*}$ )	2.7826	-0.0070	0.6115	0.6131	0.9974	0.9496	1.0000
Naive ( $\tilde{\psi}_{T^*}$ )	0.0241	0.0000	0.0122	0.0122	1.0041	0.9524	1.0080
Adjusted/debiased ( $\hat{\psi}_{T^*}$ )	0.0241	0.0000	0.0121	0.0121	1.0040	0.9522	1.0000
$n = 4,000$							
	Mean	Bias	SE	SD	SE/SD	Coverage	Rel.eff
Naive ( $\tilde{\psi}_{Y T^*}$ )	2.7859	-0.0014	0.6027	0.6028	0.9998	0.9479	1.3941
Adjusted/debiased ( $\hat{\psi}_{Y T^*}$ )	2.7860	-0.0012	0.4326	0.4324	1.0006	0.9496	1.0000
Naive ( $\tilde{\psi}_{T^*}$ )	0.0241	0.0001	0.0086	0.0087	0.9920	0.9486	1.0070
Adjusted/debiased ( $\hat{\psi}_{T^*}$ )	0.0241	0.0001	0.0086	0.0086	0.9914	0.9492	1.0000

Table 3: Power to reject either  $H_{Y|T^*}$  or  $H_{T^*}$  or both hypotheses at a nominal significance level  $\alpha = 0.025$  and with superiority/non-inferiority margins  $\delta_{Y|T^*} = \delta_{T^*} = 0$ .

	Sample size	Proposed testing procedure			Bonferroni-Holm procedure		
		$H_{Y T^*}$	$H_{T^*}$	$H_{Y T^*}$ and $H_{T^*}$	$H_{Y T^*}$	$H_{T^*}$	$H_{Y T^*}$ and $H_{T^*}$
Adjusted/debiased	500	0.5720	0.1618	0.0951	0.5320	0.1370	0.0887
Naive	500	0.3164	0.1475	0.0644	0.2889	0.1243	0.0585
Adjusted/debiased	1000	0.8744	0.2910	0.2524	0.8483	0.2740	0.2462
Naive	1000	0.5896	0.2787	0.1833	0.5511	0.2459	0.1738
Adjusted/debiased	2000	0.9943	0.5113	0.5081	0.9918	0.5105	0.5075
Naive	2000	0.8904	0.5026	0.4560	0.8674	0.4894	0.4498
Adjusted/debiased	4000	1.0000	0.8021	0.8021	1.0000	0.8021	0.8021
Naive	4000	0.9957	0.7941	0.7909	0.9949	0.7934	0.7908

Table 4: Type 1 error for testing  $H_{Y|T^*} \cap H_{T^*}$ ,  $H_{Y|T^*}$ , and  $H_{T^*}$  under the global null using signed Wald tests at a nominal significance level  $\alpha = 0.025$  and with superiority/non-inferiority margins  $\delta_{Y|T^*} = \delta_{T^*} = 0$ .

	Sample size	$H_{Y T^*} \cap H_{T^*}$	$H_{Y T^*}$	$H_{T^*}$
Adjusted/debiased	500	0.0248	0.0249	0.0250
Naive	500	0.0247	0.0271	0.0253
Adjusted/debiased	1000	0.0246	0.0256	0.0250
Naive	1000	0.0258	0.0256	0.0248
Adjusted/debiased	2000	0.0241	0.0243	0.0242
Naive	2000	0.0258	0.0251	0.0242
Adjusted/debiased	4000	0.0243	0.0243	0.0248
Naive	4000	0.0256	0.0250	0.0244

of 20000 simulated data sets are shown in Table 5.

Table 5: Simulation results based on 20,000 replications in a scenario with stronger covariate effect on the cause-specific hazard for the primary event.

	Mean	Bias	SE	SD	SE/SD	Coverage	Rel.eff
Naive ( $\tilde{\psi}_{Y T^*}$ )	2.1252	-0.0111	0.8388	0.8407	0.9977	0.9494	1.2502
Adjusted/debiased ( $\hat{\psi}_{Y T^*}$ )	2.1335	-0.0028	0.6713	0.6725	0.9982	0.9510	1.0000
Naive ( $\tilde{\psi}_{T^*}$ )	0.0361	-0.0001	0.0185	0.0186	0.9908	0.9488	1.4025
Adjusted/debiased ( $\hat{\psi}_{T^*}$ )	0.0361	-0.0001	0.0132	0.0133	0.9896	0.9480	1.0000

From Table 5 we note that efficiency gains for both estimators are now substantial with approximately 40% larger standard errors for the Aalen-Johansen estimator compared to the efficient estimator  $\psi_{T^*}$ . This simulation demonstrates that the efficiency gains in a realistic setting can be considerable for both target parameters.

## 6 Application

The FLOW (Evaluate Renal Function with Semaglutide Once Weekly) clinical kidney outcome trial randomised 3,533 patients 1:1 to receive either placebo or semaglutide on top of standard of care (Perkovic et al., 2024). Semaglutide is a glucagon-like peptide-1 (GLP-1) approved for treatment of type 2 diabetes. All patients had type 2 diabetes and had high-risk chronic kidney disease. High risk kidney disease patients were selected according to the estimated glomerular filtration rate (eGFR) per serum creatinine and urinary albumin to creatinine ratio (UACR). The trial duration was 5 years with a median follow-up time of 3.4 years. The trial objective was to demonstrate that semaglutide delayed the progression of kidney impairment and lowered the risk of kidney and cardiovascular mortality compared to placebo, both added to standard-of-care, in subjects with type 2 diabetes and chronic kidney disease (Rossing et al., 2023). The primary endpoint was time to first composite major kidney disease event consisting of; a sustained decline in eGFR above 50 % relative to baseline, sustained eGFR  $< 15$  mL/min/1.73m<sup>2</sup>, renal replacement therapy (dialysis or transplantation), renal or cardiovascular death. The annual rate of change in eGFR from randomisation, total eGFR slope, was a confirmatory secondary endpoint. The trial was event driven and employed a group sequential design with a planned interim for efficacy after two thirds of the primary endpoint events had occurred. The trial was stopped at interim following the interim evaluation.

For this application, the eGFR measurement at landmark year 2 after randomization will constitute the surrogate marker. A higher eGFR is indicative of a better renal function with an

eGFR of more than 90 mL/min/1.73m<sup>2</sup> indicating a normal or high kidney function (Stevens et al. (2024)). Thus,  $\psi_{Y|T^*} = \mathbb{E}[Y^{(1)} | T^{*(1)} > \tau] - \mathbb{E}[Y^{(0)} | T^{*(0)} > \tau] > 0$  corresponds to a positive semaglutide treatment effect on eGFR and accordingly we test the null-hypothesis:

$$H_{Y|T^*} : \psi_{Y|T^*} \leq 0.$$

Moreover, time to first major kidney disease event will constitute the terminal event of interest with non-cardiovascular and non-renal death acting as a competing risk. A lower risk of having a major kidney disease event two years after randomization corresponds to a beneficial effect of treatment (under the implicit assumption that the competing risk is not increased by treatment). Thus  $\psi_{T^*} = \mathbb{P}(T^{*(0)} \leq \tau, \epsilon^{*(0)} = 1) - \mathbb{P}(T^{*(1)} \leq \tau, \epsilon^{*(1)} = 1) > 0$  corresponds to a beneficial effect of semaglutide on risk of having a major kidney disease event. We therefore also test the null-hypothesis:

$$H_{T^*} : \psi_{T^*} \leq 0.$$

We estimate  $\psi_{Y|T^*}$  and  $\psi_{T^*}$  using the developed methodology and based on the same nuisance models that we applied in the simulation study. Next we test the hypotheses  $H_{Y|T^*}$  and  $H_{T^*}$  using the proposed closed testing strategy. The results of this analysis of the FLOW data are presented in Table 6.

Table 6: Analysis results based on FLOW trial data.

<b>On surrogate marker, eGFR at year 2 (<math>\tau = 2</math>)</b>				
		Estimate	95 % CI	P-value
Placebo:	$\theta_{Y T^*}^{(0)} = \mathbb{E}[Y^{(0)}   T^{*(0)} > \tau]$	40.419	[39.608 ; 41.231]	-
Sema:	$\theta_{Y T^*}^{(1)} = \mathbb{E}[Y^{(1)}   T^{*(1)} > \tau]$	43.618	[42.807 ; 44.429]	-
Sema - Placebo:	$\psi_{Y T^*} = \theta_{Y T^*}^{(1)} - \theta_{Y T^*}^{(0)}$	3.198	[2.232 ; 4.164]	< 0.0001
<b>On terminal event, major kidney disease events</b>				
		Estimate	95 % CI	P-value
Placebo:	$\theta_{T^*}^{(0)} = \mathbb{P}(T^{*(0)} \leq \tau, \epsilon^{*(0)} = 1)$	0.0948	[0.0811 ; 0.1085]	-
Sema:	$\theta_{T^*}^{(1)} = \mathbb{P}(T^{*(1)} \leq \tau, \epsilon^{*(1)} = 1)$	0.0662	[0.0546 ; 0.0778]	-
Placebo - Sema:	$\psi_{T^*} = \theta_{T^*}^{(0)} - \theta_{T^*}^{(1)}$	0.0286	[0.0107 ; 0.0464]	0.0017
<b>One-sided tests: Signed Wald test</b>				
	Hypothesis	Test-statistic	P-value	
Sema - Placebo:	$H_{Y T^*} : \psi_{Y T^*} \leq 0$	42.107	< 0.0001	
Placebo - Sema:	$H_{T^*} : \psi_{T^*} \leq 0$	9.821	0.0008	
<b>Intersection test: Signed Wald intersection test</b>				
	Hypothesis	Test-statistic	P-value	
Sema vs. Placebo:	$H_{Y T^*} \cap H_{T^*}$	47.769	< 0.0001	

From Table 6 we conclude that there is evidence of a clear benefit of semaglutide in lowering the risk of major kidney events after two years of treatment. In addition to this there is evidence of a clear benefit of semaglutide on kidney function in terms of increased eGFR after two years of treatment among those that are still alive and without major kidney events.

As already noted our claim of treatment benefit on major kidney events hinges on the assumption that the competing events non-cardiovascular and non-renal death are not increased by treatment. To address this assumption we perform an additional analysis in which we estimate

the change in risk of non-cardiovascular and non-renal death after two years of treatment. Such an estimate can be obtained in exactly the same manner as when estimating  $\psi_{T^*}$  based on the one-step estimator. The resulting estimated risk difference was 0.003 ( 95% CI: [-0.009; 0.015]) indicating no evidence of increased risk due to treatment.

## 7 Discussion

Current practice to analyse decline in eGFR involves very explicit modelling of eGFR profiles by means of random slope models (Vonesh et al., 2019). Such simplifications may be hard to justify in studies such as the FLOW study. This may lead to inadequate description of the actual behavior and consequent loss of power to detect a relevant decline in eGFR (DeVries et al., 2024). Moreover, effects reported from these models are based on extrapolation beyond terminal events and thus consider the impact of treatment in a hypothetical scenario where terminal events can be prevented (Kahan et al., 2020). Finally, the random slope models that are used require intensive sampling of eGFR and as such pose a burden for both study sponsors and study participants. In this paper we have offered an alternative approach to analyse eGFR that does not require such strict assumptions and we have shown by simulation and example this that approach is attractive in terms of performance and precision.

Our approach does not make explicit assumptions around the decline in eGFR or the time to terminal event. However, it still hinges on two explicit assumptions (A4) and (A5) about missing eGFR values and censoring at landmark visit. A natural extension of these assumptions would be to also condition on baseline covariates  $X$ , that is, instead consider:

(A4') Alternative Missing at random (outcome):  $Y \perp\!\!\!\perp R \mid T^* \geq \tau, A, X$

(A5') Alternative independent censoring (time to event)  $T^* \perp\!\!\!\perp C \mid A, X$

Future work evolves around extending the estimation procedure in this paper to accommodate this new set of missing data assumptions. For the specific models we fitted on the missing data mechanisms in the FLOW study to set up our simulation study there was no indication that these were associated with  $X$ . Consequently it seems that assumptions (A4) and (A5) are adequate in the context of analysing FLOW data.

In our exposition we focussed on a formalized assessment of treatment effects on one clinical score and one specific type of terminal event. However, the estimation procedure is easily extended to cover more clinical scores and and more than one type of terminal event. To also extend the testing procedure we would need to consider a generalized version of the signed Wald test (9) for the intersection hypotheses. Specifically, in our scenario we may rewrite (9) as:

$$\inf_{u \in W_1 \cap W_2} \|\hat{u} - u\|^2,$$

where  $W_j = \{u : \sqrt{\Sigma_j}u \leq 0\}$ ,  $j = 1, 2$  denote the half-spaces encoded by the constraint  $\sqrt{\Sigma}u \leq 0$ . With this rewrite it is easy to express the signed Wald test for the intersection of multiple superiority/non-inferiority hypotheses  $\{H_l\}_{l=1, \dots, L}$  as:

$$SW_{n, \cap_{l=1}^L H_l} = \inf_{u \in \cap_{j=1}^J W_j} \|\hat{u} - u\|^2, \quad (12)$$

where again  $W_j = \{u : \sqrt{\Sigma_j}u \leq 0\}$ ,  $j = 1, \dots, J$  denote the half-spaces encoded by the constraint  $\sqrt{\Sigma}u \leq 0$ .

There is no closed form expression to calculate the  $SW_{n, \cap_{l=1}^L H_l}$  in general. However, since the right hand side of 12 is identified as the minimal distance from a point to an intersection of half-spaces it can be computed numerically by Dykstras projection algorithm (Dykstra, 1983). This effectively means that we can simulate the null-distribution of the signed Wald test for all intersection hypotheses needed to enable a generalized closed testing procedure. Specifically we

can simulate the null distribution by repeatedly simulating zero mean standard normal variables  $U_i$  and calculating their distance to the intersection of half-spaces. We plan to investigate this proposal in more detail in future works.

From a FLOW perspective the above extension would facilitate that we could also provide a formalized evaluation of the impact of treatment on risk of non-cardiovascular and non-renal death.

We would also like to note that in our framework change from baseline in clinical scores and actual clinical score values at a landmark time can not be used interchangeably. For instance, in FLOW, a baseline measurement  $X_1$  of the eGFR score is available. It would therefore be natural to move from assessing treatment effect on the eGFR score  $Y$  at a landmark time to use  $\tilde{Y} = Y - X_1$  for that assessment. Note however that in our setup this would lead to contrasting

$$\begin{aligned}\psi_{\tilde{Y}|T^*} &= \mathbb{E}[\tilde{Y}^{(1)} | T^{*(1)} > \tau] - \mathbb{E}[Y^{(0)} | T^{*(0)} > \tau] \\ &= \psi_{Y|T^*} - \{\mathbb{E}[X_1 | T^* > \tau, A = 1] - \mathbb{E}[X_1 | T^* > \tau, A = 0]\}.\end{aligned}$$

Since the last term on the right hand side above is not guaranteed to be zero unless  $X_1$  is independent of  $I(T^* > \tau)$  given  $A$  we are effectively targeting another parameter to assess effect. This means that estimated treatment effects based on either  $Y$  or  $\tilde{Y}$  are not comparable due to the selection process instated by truncation.

Finally, we would like to emphasize that the developed methodology has potential to be used in many other disease areas besides chronic kidney disease. Examples of other areas where we see a potential for this methodology include KCCQ scores in heart failure patients (Spertus et al., 2020) and MOCA scores in dementia patients (Davis et al., 2021).

## References

- Blanche, P. F., Holt, A., and Scheike, T. H. (2023). On logistic regression with right censored data, with or without competing risks, and its use for estimating treatment effects. *Lifetime Data Analysis*, 29(2):441–482.
- Chan, K. C. G. and Wang, M.-C. (2010). Backward estimation of stochastic processes with failure events as time origins. *The Annals of Applied Statistics*, 4(3):1602 – 1620.
- Chernozhukov, V., Newey, W. K., and Robins, J. (2018). Double/de-biased machine learning using regularized riesz representers.
- Davis, D., Creavin, S., Yip, J., Noel-Storr, A., Brayne, C., and Cullum, S. (2021). Montreal cognitive assessment for the detection of dementia. *Cochrane Database of Systematic Reviews*, (7).
- DeVries, T., Carroll, K. J., and Lewis, S. A. (2024). A practical guide to the appropriate analysis of egfr data over time: A simulation study. *Pharmaceutical Statistics*, 23(5):742–762.
- Diggle, P., Zeger, S., Liang, K.-Y., and Heagerty, P. (2002). *Analysis of longitudinal data*. Oxford statistical science series. Oxford University Press, 2nd ed. edition.
- Dykstra, R. L. (1983). An algorithm for restricted least squares regression. *Journal of the American Statistical Association*, 78(384):837–842.
- Fitzmaurice, G. M. and Laird, N. M. (2000). Generalized linear mixture models for handling nonignorable dropouts in longitudinal studies. *Biostatistics*, 1(2):141–156.
- Frangakis, C. E., Rubin, D. B., An, M.-W., and MacKenzie, E. (2007). Principal stratification designs to estimate input data missing due to death. *Biometrics*, 63(3):641–649.
- Hines, O., Dukes, O., Diaz-Ordaz, K., and Vansteelandt, S. (2022). Demystifying statistical learning based on efficient influence functions. *The American Statistician*, pages 1–13.

- Holst, K. K. and Nordland, A. (2024). *targeted: Targeted Inference*. R package version 0.6.
- Holst, K. K. and Scheike, T. (2024). *mets: Analysis of Multivariate Event Times*. R package version 1.3.4.
- Kahan, B. C., Morris, T. P., White, I. R., Tweed, C. D., Cro, S., Dahly, D., Pham, T. M., Esmail, H., Babiker, A., and Carpenter, J. R. (2020). Treatment estimands in clinical trials of patients hospitalised for covid-19: ensuring trials ask the right questions. *BMC Medicine*, 18(286).
- Kurland, B. F. and Heagerty, P. J. (2005). Directly parameterized regression conditioning on being alive: analysis of longitudinal data truncated by deaths. *Biostatistics*, 6(2):241–258.
- Kurland, B. F., Johnson, L. L., Egleston, B. L., and Diehr, P. H. (2009). Longitudinal Data with Follow-up Truncated by Death: Match the Analysis Method to Research Aims. *Statistical Science*, 24(2):211 – 222.
- Laan, M. J. v. d. and Robins, J. M. (2003). *Unified methods for censored longitudinal data and causality*. Springer series in statistics. New York : Springer.
- Lin, D. Y. (2003). Regression analysis of incomplete medical cost data. *Statistics in Medicine*, 22(7):1181–1200.
- Marcus, R., Peritz, E., and Gabriel, K. R. (1976). On closed testing procedures with special reference to ordered analysis of variance. *Biometrika*, 63(3):655–660.
- Perkovic, V., Tuttle, K. R., Rossing, P., Mahaffey, K. W., Mann, J. F., Bakris, G., Baeres, F. M., Idorn, T., Bosch-Traberg, H., Lausvig, N. L., and Pratley, R. (2024). Effects of semaglutide on chronic kidney disease in patients with type 2 diabetes. *New England Journal of Medicine*, 391(2):109–121.
- Putter, H., Fiocco, M., and Geskus, R. B. (2007). Tutorial in biostatistics: competing risks and multi-state models. *Statistics in Medicine*, 26(11):2389–2430.
- Robertson, T., Wright, F., and Dykstra, R. (1988). *Order Restricted Statistical Inference*. Probability and Statistics Series. Wiley.
- Rossing, P., Baeres, F. M. M., Bakris, G., Bosch-Traberg, H., Gislum, M., Gough, S. C. L., Idorn, T., Lawson, J., Mahaffey, K. W., Mann, J. F. E., Mersebach, H., Perkovic, V., Tuttle, K., Pratley, Richard, o. b. o. t. F. S. C., and Investigators, F. T. (2023). The rationale, design and baseline data of flow, a kidney outcomes trial with once-weekly semaglutide in people with type 2 diabetes and chronic kidney disease. *Nephrology Dialysis Transplantation*, 38(9):2041–2051.
- Silvapulle, M. J. (1992). Robust wald-type tests of one-sided hypotheses in the linear model. *Journal of the American Statistical Association*, 87(417):156–161.
- Spertus, J. A., Jones, P. G., Sandhu, A. T., and Arnold, S. V. (2020). Interpreting the kansas city cardiomyopathy questionnaire in clinical trials and clinical care: Jacc state-of-the-art review. *Journal of the American College of Cardiology*, 76(20):2379–2390.
- Stevens, P. E., Ahmed, S. B., Carrero, J. J., Foster, B., Francis, A., Hall, R. K., Herrington, W. G., Hill, G., Inker, L. A., Kazancioğlu, R., et al. (2024). Kdigo 2024 clinical practice guideline for the evaluation and management of chronic kidney disease. *Kidney international*, 105(4):S117–S314.
- Tsiatis, A. (2006). *Semiparametric Theory and Missing Data*. Springer Series in Statistics. Springer New York.
- Vonesh, E., Tighiouart, H., Ying, J., Heerspink, H. L., Lewis, J., Staplin, N., Inker, L., and Greene, T. (2019). Mixed-effects models for slope-based endpoints in clinical trials of chronic kidney disease. *Statistics in Medicine*, 38(22):4218–4239.
- Zhang, M., Tsiatis, A. A., and Davidian, M. (2008). Improving efficiency of inferences in randomized clinical trials using auxiliary covariates. *Biometrics*, 64(3):707–715.



## A Software implementation

Installation of R package

```
> repo <- "https://kkholst.github.io/target/pkg/"
> remotes::install_cran("targeted", repos=repo)

> library("targeted")
```

Loading required package: lava

Loading required package: survival

### A.1 Simulation setup

```
> ## Treatment assignment
> p.a <- 0.5
> ## SGLT2 at baseline
> p.x2 <- 0.156
> ## eGFR at baseline
> m.x1 <- list("x2=0" = 46.24, "x2=1" = 51.15)
> s.x1 <- list("x2=0" = 14.99, "x2=1" = 15.33)
> ## eGFR at landmark
> b.y <- list(
+   "a=0" = c(40.141, 0.895, 1.993),
+   "a=1" = c(43.121, 0.863, 2.620)
+ )
> s.y <- list("a=0" = 11.85, "a=1" = 12.16)
> ## Censoring
> b.e0 <- list(
+   "a=0" = c(log(0.00014), 0, 0),
+   "a=1" = c(log(9.35e-5), 0, 0)
+ )
> gamma.e0 <- list("a=0" = 6.691, "a=1" = 6.946)
> ## Primary event
> b.e1 <- list(
+   "a=0" = c(log(0.0285), -0.0243, -0.5832),
+   "a=1" = c(log(.01817), -0.0289, -0.1261)
+ )
> gamma.e1 <- list("a=0" = 1.822, "a=1" = 1.901)
> ## Death other causes
> b.e2 <- list(
+   "a=0" = c(log(0.0154), -0.0205, -0.4549),
+   "a=1" = c(log(0.0160), 0.00687, -0.598)
+ )
> gamma.e2 <- list("a=0" = 1.143, "a=1" = 1.071)
> ## Missing data mechanism
> b.r <- list(
+   "a=0" = c(2.243, 0, 0),
+   "a=1" = c(2.309, 0, 0)
+ )
> pars <- list(
+   a = p.a,
+   x1 = list(m = m.x1, sd = s.x1),
+   x2 = p.x2,
```

```

+   y = list(m = b.y, sd = s.y),
+   r = b.r,
+   t0 = list(m = b.e0, shape = gamma.e0),
+   t1 = list(m = b.e1, shape = gamma.e1),
+   t2 = list(m = b.e2, shape = gamma.e2)
+ )
>
>
> simdata <- function(n, # sample-size
+                       parameters = pars, # model parameter
+                       tau = 2, # landmark time
+                       null = FALSE
+                       ) {
+   a <- rbinom(n, 1, parameters[["a"]]) # treatment variable
+   x2 <- rbinom(n, 1, parameters[["x2"]]) # SGL2 treatment at baseline
+   x1 <- rnorm(n, # eGFR at baseline
+     mean = with(parameters[["x1"]], m[["x2=0"]] * (1 - x2) + m[["x2=1"]] * x2),
+     sd = with(parameters[["x1"]], sd[["x2=0"]] * (1 - x2) + sd[["x2=1"]] * x2)
+   )
+   mean.x1 <- with(parameters[["x1"]], m[["x2=0"]] * (1 - parameters[["x2"]]) +
+     m[["x2=1"]] * parameters[["x2"]])
+
+   placebo <- "a=0"
+   active <- ifelse(null, "a=0", "a=1")
+   # Design matrix
+   X <- cbind(1, x1 - mean.x1, x2)
+   # Latent clinical outcome (eGFR)
+   y0 <- rnorm(n,
+     mean = with(parameters[["y"]], X %>% m[[placebo]] * (1 - a) +
+       X %>% m[[active]] * a),
+     sd = with(parameters[["y"]], sd[[placebo]] * (1 - a) + sd[[active]] * a)
+   )
+   sim_weibull <- function(X, a, gamma, b) {
+     shape <- gamma[[placebo]] * (1 - a) + gamma[[active]] * a
+     lp <- X %>% b[[placebo]] * (1 - a) + X %>% b[[active]] * a
+     rweibull(n, shape = shape, scale = exp(lp / -shape))
+   }
+   # latent censoring time
+   t0 <- sim_weibull(X, a, parameters[["t0"]]$shape, parameters[["t0"]]$m)
+   # latent event time
+   t1 <- sim_weibull(X, a, parameters[["t1"]]$shape, parameters[["t1"]]$m)
+   # latent competing death event time
+   t2 <- sim_weibull(X, a, parameters[["t2"]]$shape, parameters[["t2"]]$m)
+   failure.time <- pmin(t1, t2)
+   time <- pmin(t0, t1, t2)
+   status <- apply(cbind(t0, t1, t2), 1, which.min) - 1
+   # Observation indicator given T>tau
+   p.r <- lava::expit(X %>% parameters[["r"]][[placebo]] * (1 - a) +
+     X %>% parameters[["r"]][[active]] * a)
+   r.tau <- rbinom(n, 1, p.r)
+   y0[failure.time < tau] <- NA
+   # Observed clinical outcome (eGFR)
+   y <- y0
+   y[r.tau == 0 & time < tau] <- NA

```

```

+ # Return combined data
+ d <- data.frame(a, x1, x2, y0, y, time, r0=r.tau,
+   r = (!is.na(y)) * 1, status, failure.time
+ )
+ return(d)
+ }

```

## A.2 Estimation procedure

```

> dat <- simdata(n = 4000)
> head(dat)

```

	a	x1	x2	y0	y	time	r0	r	status	failure.time
1	0	24.42185	0	-6.603979	-6.603979	2.5512679	1	1	1	2.5512679
2	0	60.03364	0	62.135167	62.135167	3.2936547	1	1	0	10.7026974
3	0	35.53760	0	NA	NA	0.8577574	1	0	1	0.8577574
4	1	34.15262	0	26.850871	26.850871	2.6512927	1	1	1	2.6512927
5	1	19.62862	0	NA	NA	0.3394646	1	0	1	0.3394646
6	0	54.15368	1	61.252843	61.252843	4.0906297	1	1	0	11.7937432

```

> mod1 <- predictor_glm(y ~ a * (x1 + x2))
> mod2 <- predictor_glm(r ~ a * (x1 + x2), family = binomial)
> est <- estimate_truncatedscore(
+   data = dat,
+   mod.y = mod1,
+   mod.r = mod2,
+   mod.a = a ~ 1,
+   mod.event = timereg::Event(time, status) ~ a * (x1+x2),
+   time = 2,
+   cens.code = 0,
+   cause = 1
+ )
>
> est

```

	Estimate	Std.Err	2.5%	97.5%	P-value
E(Y T>=2,A=0)	41.15440	0.374125	40.42112	41.887667	0.000e+00
E(Y T>=2,A=1)	44.22482	0.375811	43.48824	44.961396	0.000e+00
diff	3.07042	0.438698	2.21059	3.930256	2.579e-12
-----					
Risk(T<2 A=0)	0.09931	0.006652	0.08627	0.112343	2.150e-50
Risk(T<2 A=1)	0.07807	0.005984	0.06635	0.089804	6.628e-39
riskdiff	-0.02123	0.008901	-0.03868	-0.003785	1.707e-02

```

> s <- summary(est, noninf.y = 0, noninf.t = -0.05, alpha = 0.05)
> s

```

```

-- Parameter estimates -----

```

	Estimate	Std.Err	2.5%	97.5%	P-value
E(Y T>=2,A=0)	41.15440	0.374125	40.42112	41.887667	0.000e+00
E(Y T>=2,A=1)	44.22482	0.375811	43.48824	44.961396	0.000e+00
diff	3.07042	0.438698	2.21059	3.930256	2.579e-12
-----					
Risk(T<2 A=0)	0.09931	0.006652	0.08627	0.112343	2.150e-50
Risk(T<2 A=1)	0.07807	0.005984	0.06635	0.089804	6.628e-39
riskdiff	-0.02123	0.008901	-0.03868	-0.003785	1.707e-02

-- One-sided tests -----

b1 =  $E(Y|T \geq 2, A=1) - E(Y|T \geq 2, A=0)$

Signed Wald Test

data: H1:  $b1 \leq 0$   
Q = 48.985, p-value = 1.289e-12  
alternative hypothesis: HA1:  $b1 > 0$   
sample estimates:  
    b1  
3.070424

--

b2 =  $\text{Risk}(T < 2 | A=0) - \text{Risk}(T < 2 | A=1)$

Signed Wald Test

data: H2:  $b2 \leq -0.05$   
Q = 64.043, p-value = 6.087e-16  
alternative hypothesis: HA2:  $b2 > -0.05$   
sample estimates:  
    b2  
0.02123067

-- Intersection test -----

Signed Wald Intersection Test

data:  $H1 \wedge H2$   
Q = 129.95, p-value < 2.2e-16

-----  
Extracting the test statistics and p-values in a matrix-form

> *parameter(s)*

	estimate	statistic	p.value
b1	3.07042397	48.98532	1.289426e-12
b2	0.02123067	64.04278	6.087319e-16
intersection	NA	129.94584	1.852904e-29